

Electronic Supporting Information

Photocatalytic Hydrogen Generation Coupled to Pollutant Utilisation Using Carbon Dots Produced from Biomass

Demetra S. Achilleos^{a,†}, Hatice Kasap^a and Erwin Reisner^{a,*}

^aChristian Doppler Laboratory for Sustainable SynGas Chemistry, Department of Chemistry, University of Cambridge, Lensfield Road, Cambridge CB2 1EW (UK)

† Present Address: School of Chemistry, University College Dublin, Science Centre South, Belfield, Dublin 4.

*Corresponding author: reisner@ch.cam.ac.uk

Table S1. Simultaneous photocatalytic H₂ evolution and pollutant utilisation in synthetic water^a

Entry	Photocatalytic materials	Co-catalyst	Reaction medium	Targeted pollutants and/or SED	H ₂ / μmol	Activity/μmol H ₂ g ⁻¹ h ⁻¹	Ref.
1	F-TiO ₂ ^c /Pt, P-TiO ₂ ^d /Pt	Pt	Synthetic water	4-chlorophenol, urea	~5.0–20.0 ^b	67.0–267.0	S1,2
2	TiO ₂ –Pt	Pt	Synthetic water	Oxalic acid	~10.0 ^b	500.0	S3
3	TiO ₂ –Pt	Pt	Synthetic water	Acetic acid	~0.0 ^b	0.0	S4
4	Reduced TiO ₂ nanodots coated graphite-like carbon spheres	Pt	Synthetic water	Rhodamine B, methylene blue, 4-chlorophenol, ciprofloxacin	—	255.2	S5
5	TiO ₂ –Pt–CdS	Pt	Synthetic water	Ethanol	~21.0 ^g	~37.7 ^g	S6
6	Mn-N-TiO ₂ –g-C ₃ N ₄ –graphene QDs ^e	Pt	Synthetic water	p-nitrophenol, diethyl phthalate, ciprofloxacin	—	900.0–1500.0	S7
7	CuO/nano-TiO ₂	n. d. ^f	Simulated sea water	Oxalic acid	—	~ 2.0	S8
8	TiO ₂ –Au	Au	Regional river sources in Ontario and Quebec (34 °C)	n. d. ^f	—	8.0–28.0	S9
9	C/X-TiO ₂ –C ₃ N ₄ NTs (X = N, F, Cl)	Pt	Synthetic water	p-chlorophenol, rhodamine B, triethylamine	~1.2–8.0	~2.0–13.3	S10
10	MoS ₂ –TiO ₂	MoS ₂	Simulated sea water	MeOH	—	380000 ^h	S11
11	α-cellulose CDs	NiP	Untreated sea water	EDTA	17.3 ^k	13659.8 ^l	This work
12	α-cellulose CDs	NiP	Untreated river water	EDTA	13.8 ^k	2129.6 ^k	This work
13	α-cellulose CDs	NiP	Synthetic water	Prometryn	5.8 ^k	602.6 ^k	This work

^aThese systems employ purified water enriched with pollutants (synthetic water) and thus ignore significant light attenuation effects from highly concentrated organic substances (i.e. humic compounds due to plant decomposition), which often exist at higher quantities than the pollutants¹²; ^bH₂ evolution reported at pH 6 (similar to our photocatalytic systems, entries 11–13); ^cF-TiO₂: TiO₂ modified with fluoride anions; ^dP-TiO₂: TiO₂ modified with phosphate anions; ^eQDs: quantum dots; ^fn. d.: not defined; ^gSpecific activity in the presence of ethanol (0.05 μmol min⁻¹) with 80 mg photocatalyst; ^hoverestimated activity calculated upon neglecting the mass of TiO₂ in the sample (only MoS₂ mass was accounted); ^kphotocatalysis at 2.2 mg α-cellulose CDs; ^lphotocatalysis at 0.03 mg α-cellulose CDs.

Table S2. Photocatalytic systems for separate H₂ evolution under inert conditions and pollutant degradation under air^a

Entry	Photocatalytic materials	Co-catalyst	SED for HER	Reaction medium	Targeted Pollutants	H ₂ / μmol	Activity/μmol H ₂ g ⁻¹ h ⁻¹	Ref.
1	<i>g</i> -C ₃ N ₄ –Ag–MoS ₂	MoS ₂	TEOA ^b	Purified water	Rhodamine B	–	~100.0	S13
2	ZnIn ₂ S ₄ – <i>g</i> -C ₃ N ₄	–	Trolamine	Purified water	Methyl orange, phenol	–	953.5	S14
3	Petal-like CdS–S-doped C ₃ N ₄	–	Lactic acid	Purified water	Rhodamine B, bisphenol A	–	248.0	S15
4	C ₃ N ₄ with Al-Coordination Sites	Pt	TEOA	Purified water	4-Chlorophenol	–	12000	S16
5	Zn ₃ In ₂ S ₆ /fluorinated polymeric C ₃ N ₄ nanosheets	Pt	Na ₂ SO ₃ /Na ₂ S	Purified water	Methyl orange	–	510.8	S17
6	Bi ₂ WO ₆ /Cu _{1.8} Se	Au, Pt	Na ₂ SO ₃ /Na ₂ S	Purified water	Congo red	–	82.0	S18
7	TiO ₂ NPs–TiO ₂ nanowires	–	Methanol	Purified water	Rhodamine B	–	19.0	S19
8	Polyoxometalate-based Zr-MOFs	–	Methanol	Purified water	Rhodamine B	–	72.7	S20
9	α-cellulose CDs	NiP	EDTA	Purified water	EDTA	15.6 ^c	13451.8 ^d	This work

^aH₂ evolution takes place in the presence of a co-catalyst and a sacrificial electron donor (SED) under inert conditions, whereas pollutant degradation is driven by reactive hydroxyl species as it occurs under air without fuel production; ^bTEOA: triethanolamine; ^cphotocatalysis at 2.2 mg α-cellulose;

^dphotocatalysis at 0.03 mg α-cellulose CDs.

Table S3. Photocatalytic systems for pollutant degradation only (without H₂ production)^a

Entry	Photocatalytic materials	Pollutants	Method	Ref.
1	Au NPs ^b –ZnO nanorods	4-Chlorophenol	Photocatalysis	S21
2	Nano-TiO ₂ –Pyrex glass	Methyl parathion, lindane, dichlorvos	Photocatalysis	S22
3	TiO ₂ NPs	Alachlor, fenitrothion	Photocatalysis	S23
4	Ag–AgBr–Al ₂ O ₃	2-Chlorophenol, 2,4-dichlorophenol, trichlorophenol	Photocatalysis	S24
5	TiO ₂ NPs–γ-Fe ₂ O ₃	Propachlor	Photocatalysis	S25
6	Ti-doped β-Bi ₂ O ₃	Pentachlorophenol	Photocatalysis	S26
7	Au–Pd–TiO ₂ nanotube film	Malathion	Photocatalysis	S27
8	TiO ₂ nanowire	Atrazine, fluoxetine, venlafaxin, lincomycin, sulfamethoxazole, diclofenac, bisphenol A, gemfibrozil, trimethoprim	Photocatalysis	S28
9	TiO ₂ –MWCNTs ^c	Atrazine	Microwave-assisted photocatalysis	S29
10	Au-coated TiO ₂ nanotube array	Dichlorophenoxyacetic acid, methyl-parathion	Photocatalysis	S30
11	Bi-doped goethite–hematite nanostructures	Metalaxyl	Photo-Fenton-like process	S31
12	Fe ₃ O ₄ –mTiO ₂ –CQDs ^d	Ciprofloxacin, methylene blue, quinalphos, 4-nitrophenol	Photocatalysis	S32
13	mesoporous α-Fe ₂ O ₃ –CQDs _s	Methylene blue	Photocatalysis	S33
14	Bi ₂ WO ₆ –CQDs _s	Rhodamine B, ciprofloxacin, tetracycline hydrochloride, bisphenol A	Photocatalysis	S34
15	TiO ₂ –CDs _s	Methylene blue	Photocatalysis	S35
16	g-C ₃ N ₄ –CDs	Phenol	Photocatalysis	S36
17	Cl-functionalised CDs	Phthalocyanine	Photocatalysis	S37
18	3D ordered macroporous g-C ₃ N ₄	Rhodamine B	Photocatalysis	S38

19	<i>g</i> -C ₃ N ₄ nanofibers	Rhodamine B	Photocatalysis	S39
20	Mesoporous <i>g</i> -C ₃ N ₄	Chlorophenol, phenol	Photocatalysis	S40
21	<i>g</i> -C ₃ N ₄ –PANI ^e	Methylene blue	Photocatalysis	S41
22	Boron-doped <i>g</i> -C ₃ N ₄	Rhodamine B, methylene orange	Photocatalysis	S42
23	Phosphate-modified graphitic C ₃ N ₄	Phenol	Photocatalysis	S43
24	Graphite oxide and 2D oxidised C ₃ N ₄ nanodots	Rhodamine B	Photocatalysis	S44
25	2D porous C ₃ N ₄ nanosheets–N-doped graphene/layered MoS ₂	Methylene blue	Photocatalysis	S45
26	Boron-doped reduced graphene oxide	Rhodamine B	Photocatalysis	S46
27	Graphene oxide–PANI	Methyl orange, methylene blue, rhodamine B	Photocatalysis	S47
28	Crystalline phosphorus fibers	Rhodamine B	Photocatalysis	S48
29	TiO ₂ –red phosphorus	Rhodamine B	Photocatalysis	S49

^aThese systems solely degrade pollutants using hydroxyl radicals generated from O₂ reduction and water oxidation⁵⁰, and thus do not produce any fuel; ^bNPs: nanoparticles; ^cMWCNTs: multiwalled carbon nanotubes; ^dCQDs: carbon quantum dots; ^ePANI: polyaniline.

Table S4. T_{max}^a and RFAs^b of xylan, α -cellulose and lignin in waste biomass

Precursor	Xylan		Cellulose		Lignin	
	T_{max} / °C	RFA _x ^c	T_{max} / °C	RFA _c ^d	T_{max} / °C	RFA _l ^e
<i>G. nivalis</i>	209.6	0.21	317.7	0.55	434.0	0.23
<i>Cyprus olive tree</i>	268.1	0.30	332.4	0.43	402.8	0.27
<i>G. elliptica</i>	240.4	0.34	303.0	0.31	412.4	0.35
<i>T. baccata</i>	233.7	0.41	308.5	0.14	381.3	0.45
<i>E. X. ebbingei</i>	299.3	0.56	344.4	0.14	413.5	0.30

^a T_{max} : maximum decomposition temperature (in °C) determined by TGA; ^bRFAs: relative fractional areas calculated by TGA, defined as the ratio of the area of a single component divided by the overall areas of all components; ^cRFA_x= A_x/ A_x+ A_c+ A_l (x: xylan, c: α -cellulose, l: lignin); ^dRFA_c= A_c/ A_x+ A_c+ A_l; ^eRFA_l= A_l/ A_x+ A_c+ A_l.

Table S5. CD surface functionalities determined by XPS^a

Entry	Precursor	C1s			O1s				N1s			
		C=C	C–O	C=O	C=O	Content (%)	C–O	Content (%)	Pyrrolic	Pyridinic	N–Q	Pyridinic N ⁺ –O [–]
		BE / eV	BE / eV	BE / eV	BE / eV	BE / eV	BE / eV	BE / eV				
1	α -cellulose	284.8	286.3	288.5	531.8	89.5	534.1	10.5	-	-	-	-
2	xylan	284.7	286.2	288.3	531.3	36.9	532.7	63.1	-	-	-	-
3	lignin	284.7	286.2	288.4	531.3	30.4	532.6	69.6	-	-	-	-
4	cotton wool	284.4	286.0	288.2	531.2	78.3	532.6	21.7	-	-	-	-
5	<i>G. nivalis</i>	284.7	286.0	287.9	531.7	63.6	532.8	36.4	399.3	-	400.2	406.7
6	Cyprus olive tree	284.3	285.6	288.3	531.2	79.4	532.8	20.6	-	398.6	400.4	-
7	<i>G. elliptica</i>	284.7	286.1	288.4	531.3	66.7	532.9	33.3	-	398.7	400.3	-
8	<i>T. baccata</i>	284.3	286.1	288.5	531.4	60.9	533.0	39.1	399.8	-	400.3	-
9	<i>E. X. ebbingei</i>	284.8	286.5	288.1	531.7	46.3	532.8	53.7	399.1	-	400.4	-

^aCD functionalities were determined based on the binding energies (BE, eV) of the main features appeared in the C, O and N 1s XPS spectra of the photoabsorbers. Surface C–O and C=O contents were calculated based on the integrals of the main bands in the O 1s XPS spectra.

Table S6. Sizes of carbonaceous photoabsorbers by TEM

Entry	Precursor	Diameter (nm) ¹
1	α -cellulose	9.3 ± 2.9
2	xylan	114.7 ± 20.0
3	lignin	93.6 ± 3.8
4	cotton wool	8.9 ± 2.6
5	<i>G. nivalis</i>	7.1 ± 1.8
6	Cyprus olive tree	10.6 ± 3.3
7	<i>G. elliptica</i>	95.8 ± 12.0
8	<i>T. baccata</i>	44.5 ± 8.9
9	<i>E. X. ebbingei</i>	123.6 ± 27.0

¹The determination of the sizes of the photoabsorbers was based on **Figures S14-S17**.

Table S7. Photo-generated H₂ in purified water using CDs from purified biomass^a

Entry	Precursor	CDs / mg	t _{irr} / h	H ₂ / μmol	± σ / μmol	TON _{NiP} / mol H ₂ (mol NiP) ⁻¹	± σ / mol H ₂ (mol NiP) ⁻¹	Activity/ μmol H ₂ (g CDs) ⁻¹ (after 1 h)	± σ / μmol H ₂ (g CDs) ⁻¹ h ⁻¹
1	α-cellulose	0.03	6	0.9	0.04	18.7	0.8	13451.8	540.3
2			24	1.2	0.03	24.0	0.7	-	-
3	α-cellulose	0.06	6	1.7	0.02	34.8	0.4	11685.8	586.2
4			24	2.2	0.03	44.8	0.6	-	-
5	α-cellulose	0.15	6	3.4	0.10	67.5	2.1	10109.3	339.6
6			24	4.1	0.20	81.9	4.4	-	-
7	α-cellulose	0.30	6	5.4	0.05	107.9	0.9	7146.7	304.8
8			24	6.3	0.40	126.6	7.3	-	-
9	α-cellulose	0.90	6	10.5	0.20	209.1	4.4	4326.6	141.0
10			24	10.9	0.20	219.0	3.7	-	-
11	α-cellulose	2.20	6	11.0	0.50	220.1	9.8	1101.1	36.2
12			24	15.6	0.70	312.8	14.6	-	-
13	α-cellulose	2.80	6	13.4	0.40	268.2	8.8	1410.4	82.1
14			24	15.1	0.70	301.7	13.9	-	-
15	xylan	2.20	6	3.1	0.10	62.5	1.5	624.5	8.3
16			24	4.7	0.30	94.7	6.8	-	-
17	lignin	2.20	6	0.4	0.06	8.4	1.3	86.8	15.8
18			24	0.5	0.07	10.2	1.4	-	-

^aSolar-light driven (AM 1.5G, 100 mW cm⁻², 25 °C) H₂ production took place using CDs from purified biomass in the presence of NiP (50 nmol), in EDTA (0.1 M, pH 6, 3 mL) after 6 and 24 h of irradiation.

Table S8. Photocatalytic performances of metal-free carbonaceous photoabsorbers in purified water^a

Entry	Photoabsorbers	Catalyst	SED	H ₂ / μmol	Activity / μmol g ⁻¹ h ⁻¹	TON _{cat}	QE ^b / %	Ref.
1	<i>a</i> -CD	NiP	EDTA	0.6	397	64	1.4 ^c	S51
2	<i>a</i> -CD	NiP	TCEP ^f /AA ^g	10.9	53	1094	n.d.	S52
3	<i>g</i> -CD	NiP	EDTA	0.5	1,549	45	n.d.	S53
4	<i>g</i> -N-CD	NiP	EDTA	2.8	7,950	277	5.2 ^c	S53
5	CD (yeast)	Pt	TEOA ^h	n.d.	31	n.d.	n.d.	S54
6	^{NH₂} CNx	NiP	EDTA	3.3	437	166	0.4 ^d	S55
7	^{N≡C} CNx	NiP	4-MBA ^k	21.3	311	425	15.2 ^c	S56
8	<i>g</i> -C ₃ N ₄	Pt	TEOA	n.d.	20,000	641	26.5 ^e	S57
9	α -cellulose CDs	NiP	EDTA	15.6	13,451.8	312.8	11.4 ^c	This work

^aThese systems use sacrificial electron donors (SED) and non-precious (**NiP**) as well as noble-metal catalysts (Pt) in purified water; ^bQE: quantum efficiency; ^cQE measured at 360 nm; ^dQE measured at 365 nm; ^eQE measured at 400 nm; ^fTCEP: tris(carboxyethyl)phosphine; ^gAA: ascorbic acid; ^hTEOA: triethanolamine; ^k4-MBA: 4-methylbenzyl alcohol.

Table S9. Control photocatalytic experiments with and without α -cellulose CDs, EDTA and NiP^a

Entry	Reaction medium	CDs / mg	SED / 0.1 M	NiP / nmol	H ₂ / μ mol	$\pm \sigma$ / μ mol	Activity/ μ mol H ₂ (g CDs) ⁻¹ h ⁻¹ (after 1 h)	$\pm \sigma$ / μ mol H ₂ (g CDs) ⁻¹ h ⁻¹
No UV cut-off filter ($\lambda > 300$ nm)								
1	Purified water	2.2	-	50	0.1	0.01	19.0	2.8
2	Purified water	-	EDTA	50	-	-	-	-
3	Purified water	2.2	EDTA	-	-	-	-	-
4	Sea water	2.2	EDTA	-	-	-	-	-
5	River water	2.2	EDTA	-	-	-	-	-
UV cut-off filter ($\lambda > 400$ nm)								
6	Purified water	2.2	EDTA	50	4.4	0.4	233.8	11.3

^aThese experiments were carried out both in purified and untreated media, under full solar spectrum irradiation (AM 1.5 G, 100 mW cm⁻²), at 25 °C. The results in the presence of an optical filter ($\lambda > 400$ nm) with all system components are also provided, to indicate the activity of the α -cellulose CDs as visible-light photoabsorbers.

Table S10. Photocatalytic H₂ production in purified water using CDs from biomass waste^a

Entry	Precursor	CDs / mg	t _{irr} / h	H ₂ / μmol	± σ / μmol	TON _{NiP} / mol H ₂ (mol NiP) ⁻¹	± σ / mol H ₂ (mol NiP) ⁻¹	Activity/ μmol H ₂ (g CDs) ⁻¹ h ⁻¹ (after 1 h)	± σ / μmol H ₂ (g CDs) ⁻¹ h ⁻¹
1	cotton wool	2.20	6	11.8	0.3	235.0	5.9	2195.2	83.1
2			24	12.7	0.1	254.1	2.8	-	-
3	<i>G. nivalis</i>	2.20	6	6.2	0.1	123.0	2.3	847.1	10.8
4			24	8.7	0.1	174.9	2.5	-	-
5	Cyprus olive tree	2.20	6	5.3	0.3	105.9	5.6	1197.3	33.3
6			24	7.8	0.9	155.5	16.9	-	-
7	<i>G. elliptica</i>	2.20	6	4.5	0.1	89.4	0.7	746.6	25.6
8			24	6.5	0.1	129.9	0.6	-	-
9	<i>T. baccata</i>	2.20	6	3.5	0.1	70.2	1.5	569.8	84.4
10			24	4.7	0.1	93.9	2.5	-	-
11	<i>E. X. ebbingei</i>	2.20	6	3.2	0.2	63.9	3.1	684.4	16.8
12			24	3.9	0.1	79.0	2.0	-	-
13	cotton pads	2.20	6	4.9	0.2	97.4	3.4	870.0	33.5
			24	6.6	0.2	132.5	4.0	-	-
14	Cotton T-shirt	2.20	6	1.7	0.2	34.8	0.3	355.2	35.5
15			24	2.8	0.3	55.1	5.5	-	-

^aSolar driven (AM 1.5G, 100 mW cm⁻², 25 °C) H₂ production was carried out in the presence of NiP (50 nmol), in EDTA (0.1 M, pH 6, 3 mL), after 6 and 24 h of irradiation.

Table S11. Experimentally and theoretically-determined H₂ evolution yields^a

Entry	Biomass waste precursor	Photocatalytic activity / $\mu\text{mol H}_2$	
		Experimental ^a	Theoretical ^b
1	<i>G. nivalis</i>	8.7 ± 0.1	9.7
2	<i>Cyprus olive tree</i>	7.8 ± 0.9	8.2
3	<i>G. elliptica</i>	6.5 ± 0.1	6.5
4	<i>T. baccata</i>	4.7 ± 0.1	4.3
5	<i>E. X. ebbingei</i>	3.9 ± 0.1	4.9

^aExperimentally-determined H₂ evolution capacities (in μmol), as obtained from photocatalytic experiments using CDs from crude biomass; ^bTheoretically determined H₂ evolution capacities, calculated by multiplying the RFA for each component (obtained by TGA) with the capacity of the respective pure constituent to produce H₂ after 24 h of irradiation (α -cellulose; 15.6 μmol , xylan; 4.7 μmol and lignin; 0.5 μmol , **Fig. 3a**). The derived values for all components were then summed up, to result the overall activity for each plant species.

Table S12. Photoinduced H₂ production in sea water using α -cellulose- and waste biomass-derived CDs^a

Entry	Precursor	CDs / mg	t _{irr} / h	H ₂ / μmol	$\pm \sigma$ / μmol	TON _{NiP} / mol H ₂ (mol NiP) ⁻¹	$\pm \sigma$ / mol H ₂ (mol NiP) ⁻¹	Activity/ $\mu\text{mol H}_2$ (g CDs) ⁻¹ h ⁻¹ (after 1 h)	$\pm \sigma$ / $\mu\text{mol H}_2$ (g CDs) ⁻¹ h ⁻¹
1	α -cellulose	2.20	6	12.6	0.2	251.6	3.6	2072.3	50.8
2			24	17.3	1.2	345.9	24.4	-	-
3	α -cellulose	0.03	6	0.6	0.1	11.4	1.4	13659.8	120.8
4			24	1.2	0.1	23.0	0.1	-	-
5	cotton wool	2.20	6	9.7	0.5	193.8	10.3	1758.9	86.4
6			24	13.5	0.3	270.0	6.4	-	-
7	<i>G. nivalis</i>	2.20	6	9.7	0.20	193.1	3.7	1354.3	59.7
8			24	18.1	0.8	361.5	15.3	-	-
9	Cyprus olive tree	2.20	6	5.8	0.5	115.4	9.6	952.7	89.2
10			24	11.0	0.5	219.8	9.4	-	-
11	<i>G. elliptica</i>	2.20	6	4.7	0.3	94.4	5.5	790.3	23.2
12			24	8.7	0.5	173.3	9.1	-	-
13	<i>T. baccata</i>	2.20	6	3.2	0.1	63.2	2.0	612.0	26.1
14			24	5.4	0.1	108.1	1.6	-	-
15	<i>E. X. ebbingei</i>	2.20	6	2.1	0.1	42.3	0.4	357.9	7.1
16			24	3.9	0.1	77.7	1.8	-	-

^aSolar driven (AM 1.5G, 100 mW cm⁻², 25 °C) H₂ production in sea water, using CDs from α -cellulose and biomass waste in the presence of NiP (50 nmol), in EDTA (0.1 M, pH 6, 3 mL), after 6 and 24 h of irradiation.

Table S13. Solar-driven H₂ production in river water using α -cellulose- and biomass waste-derived CDs^a

Entry	Precursor	CDs / mg	t _{irr} / h	H ₂ / μmol	$\pm \sigma$ / μmol	TON _{NiP} / mol H ₂ (mol NiP) ⁻¹	$\pm \sigma$ / mol H ₂ (mol NiP) ⁻¹	Activity/ $\frac{\mu\text{mol H}_2 (\text{g CDs})}{\text{h}^{-1}}$ (after 1 h)	$\pm \sigma$ / $\frac{\mu\text{mol H}_2 (\text{g CDs})}{\text{h}^{-1}}$
1	α -cellulose	2.20	6	12.6	0.6	252.3	11.6	2129.6	174.2
2			24	13.8	0.4	275.1	7.5	-	-
3	cotton wool	2.20	6	9.6	0.2	191.8	4.2	1729.9	39.6
4			24	11.1	0.3	222.5	6.4	-	-
5	<i>G. nivalis</i>	2.20	6	5.9	0.1	117.5	2.0	1137.0	21.9
6			24	8.1	0.1	161.3	1.9	-	-
7	Cyprus olive tree	2.20	6	5.8	0.2	116.0	3.8	1297.7	24.8
8			24	8.8	0.1	176.5	1.6	-	-
9	<i>G. elliptica</i>	2.20	6	5.2	0.2	104.1	3.8	736.8	43.0
10			24	8.0	0.4	158.9	7.2	-	-
11	<i>T. baccata</i>	2.20	6	4.2	0.2	83.6	4.2	629.4	57.4
12			24	6.3	0.3	126.5	6.9	-	-
13	<i>E. X. ebbingei</i>	2.20	6	2.7	0.2	53.5	4.8	327.0	31.1
			24	4.5	0.5	89.5	9.1	-	-

^aConditions; α -cellulose- and biomass waste-derived CDs were irradiated with simulated light (AM 1.5G, 100 mW cm⁻², 25 °C) in river water, in the presence of NiP (50 nmol), in EDTA (0.1 M, pH 6, 3 mL), at 25 °C, and the results after 6 and 24 h of irradiation are listed above.

Table S14. Photo-H₂ production with α -cellulose CDs in purified, sea and river water with and without EDTA^a

Entry	Reaction medium	Electron Donor	t _{irr} / h	H ₂ / μmol	$\pm \sigma$ / μmol	TON _{NiP} / mol H ₂ (mol NiP) ⁻¹	$\pm \sigma$ / mol H ₂ (mol NiP) ⁻¹	Activity/ $\mu\text{mol H}_2$ (g CDs) ⁻¹ h ⁻¹ (after 1 h)	$\pm \sigma$ / $\mu\text{mol H}_2$ (g CDs) ⁻¹ h ⁻¹
1	Purified water	EDTA	6	11.0	0.5	220.1	9.8	1101.1	36.2
2			24	15.6	0.7	312.8	14.6	-	-
3	Purified water	-	6	0.1	0.001	2.7	0.01	19.0	2.8
4			24	0.1	0.01	2.7	0.2	-	-
5	Sea water	EDTA	6	12.6	0.2	251.6	251.6	2072.3	50.8
6			24	17.3	1.2	345.9	24.4	-	-
7	Sea water	-	6	2.9	0.5	57.0	9.4	293.6	42.8
8			24	5.6	0.4	111.3	7.2	-	-
9	River water	EDTA	6	12.6	0.6	252.3	11.6	2129.6	174.2
10			24	13.8	0.4	275.1	7.5	-	-
11	River water	-	6	3.4	0.2	67.61	4.6	230.8	11.1
12			24	5.1	0.1	102.33	1.2	-	-

^aConditions; α -cellulose CDs (2.2 mg) were irradiated (AM 1.5G, 100 mW cm⁻², 25 °C) in purified, sea and river water, in the absence and presence of EDTA (0.1 M, pH 6, 3 mL).

Table S15. Solar-H₂ generation using α -cellulose CDs with organic pollutants and chloride ions as SEDs^a

Entry	Electron Donor	t _{irr} / h	H ₂ / μmol	$\pm \sigma$ / μmol	TON _{NiP} / mol H ₂ (mol NiP) ⁻¹	$\pm \sigma$ / mol H ₂ (mol NiP) ⁻¹	Activity/ $\mu\text{mol H}_2$ (g CDs) ⁻¹ h ⁻¹ (after 1 h)	$\pm \sigma$ / $\mu\text{mol H}_2$ (g CDs) ⁻¹ h ⁻¹
1	Benzaldehyde	6	2.0	0.4	39.2	7.6	263.0	120.1
2		24	2.2	0.3	43.8	5.5	-	-
3	Atrazine	6	2.6	1.3	52.3	25.5	118.7	67.7
4		24	5.1	0.9	102.8	19.1	-	-
5	Cl ⁻	6	2.1	0.2	41.0	4.1	75.2	30.5
6		24	5.8	0.4	116.6	8.3	-	-
7	Prometryn	6	5.0	0.2	99.8	3.0	602.6	67.3
8		24	5.8	0.3	116.5	6.6	-	-
9	Terbutryn	6	3.4	0.4	67.8	7.1	382.8	33.4
10		24	4.4	0.2	88.8	3.9	-	-
11	None	6	0.1	0.001	2.7	0.01	19.0	2.8
12	None	24	0.1	0.01	2.7	0.2	-	-

^aExperiments were carried out using α -cellulose CDs in KPi (0.1 M, pH 6, 3 mL), in the absence of EDTA, but instead in the existence of organic pollutants (200 μmol) and chloride ions (3.2 wt%), found in river and sea water.

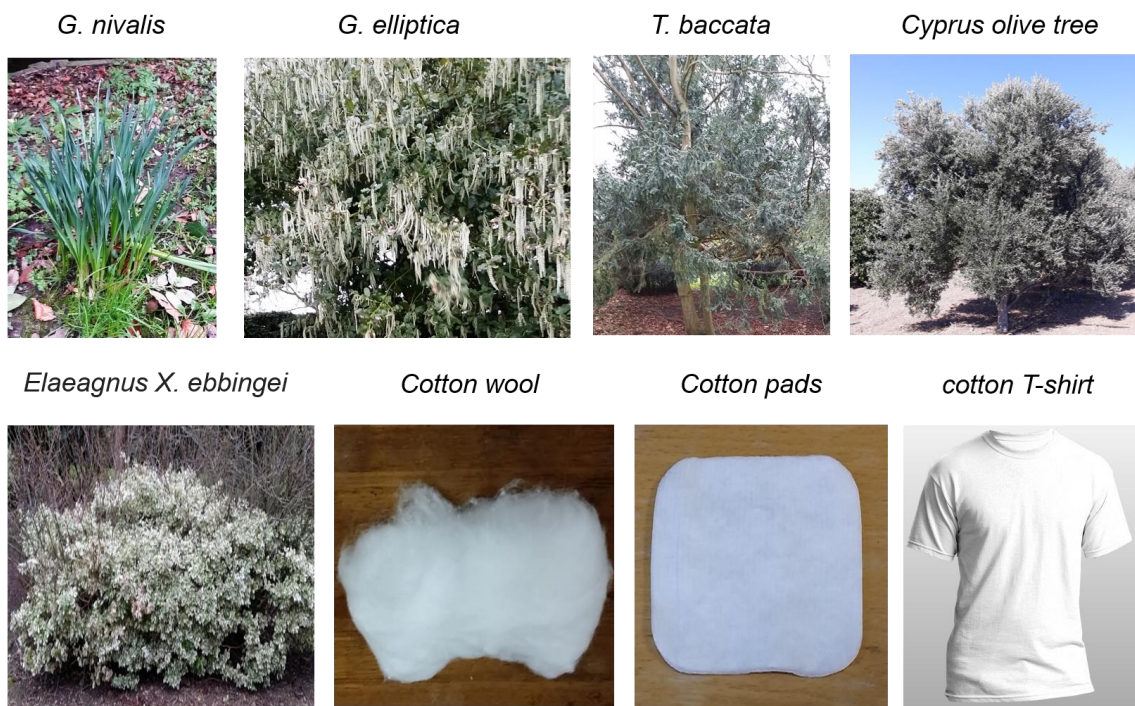


Figure S1. Photos of waste biomass samples from plants and cotton used for CD synthesis.

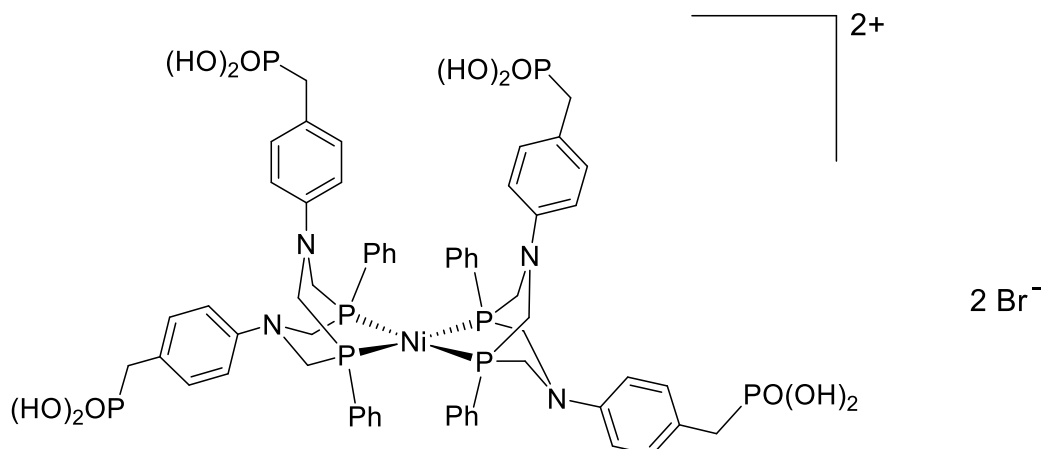


Figure S2. Chemical structure of Ni-bis(diphosphine) (**NiP**) molecular catalyst used to drive H₂ evolution under model and real-world conditions.

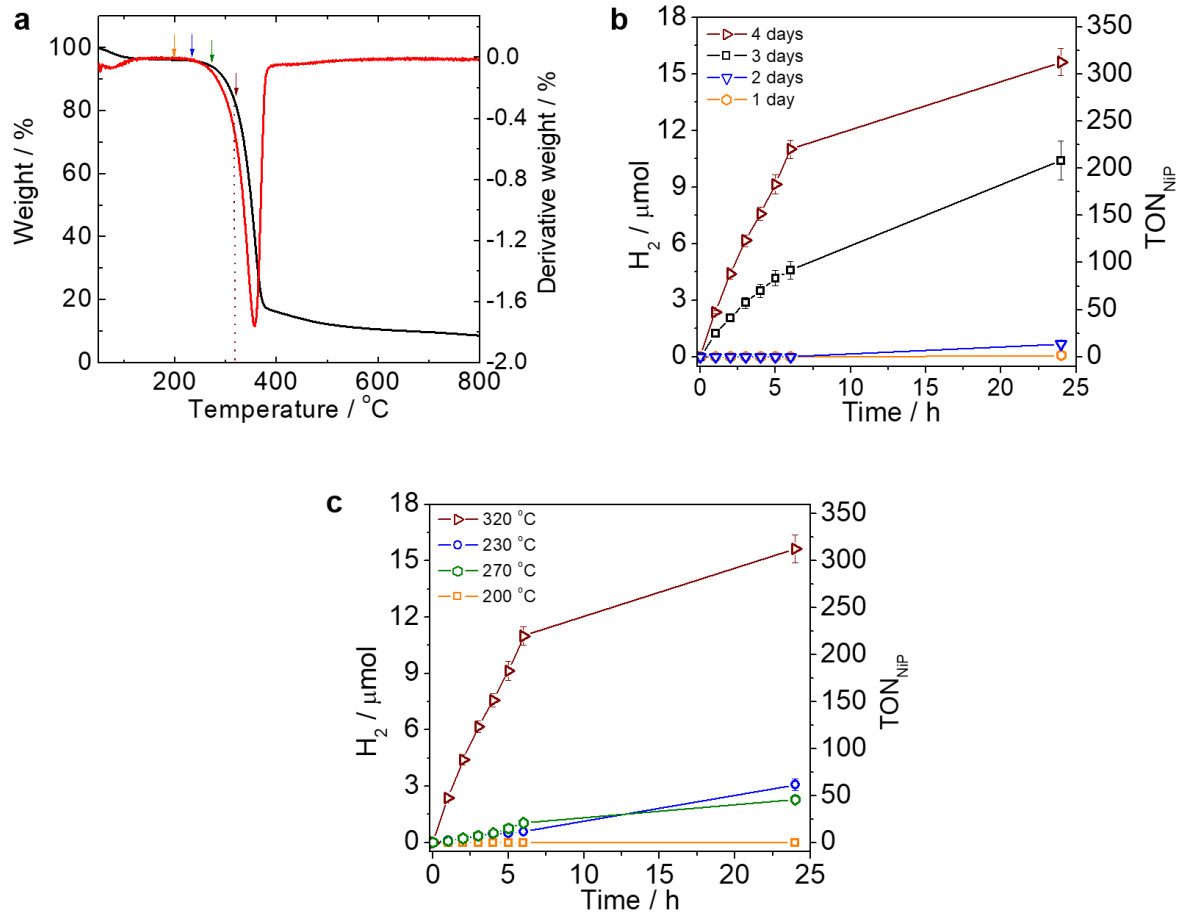


Figure S3. **a**, TGA thermogram (black) and first TGA derivative (red) of α -cellulose. The arrows indicate the temperatures at which α -cellulose was treated thermally to define the optimum calcination temperature for the synthesis of CDs. **b**, Photo-induced H_2 generation using α -cellulose photoabsorbers (2.2 mg) synthesised at different calcination times; 1, 2, 3 and 4 days at 320 °C. **c**, Solar-light driven H_2 production from α -cellulose CDs (2.2 mg) synthesised upon calcination of α -cellulose at 200, 230, 270 and 320 °C. Conditions; all experiments were carried out under full solar light irradiation (AM 1.5 G, 100 mW cm^{-2}), for 24 h, in the presence of **NiP** (50 nmol) and EDTA (0.1 M, pH 6, 3 mL), under N_2 atmosphere containing 2% CH_4 , at 25 °C.

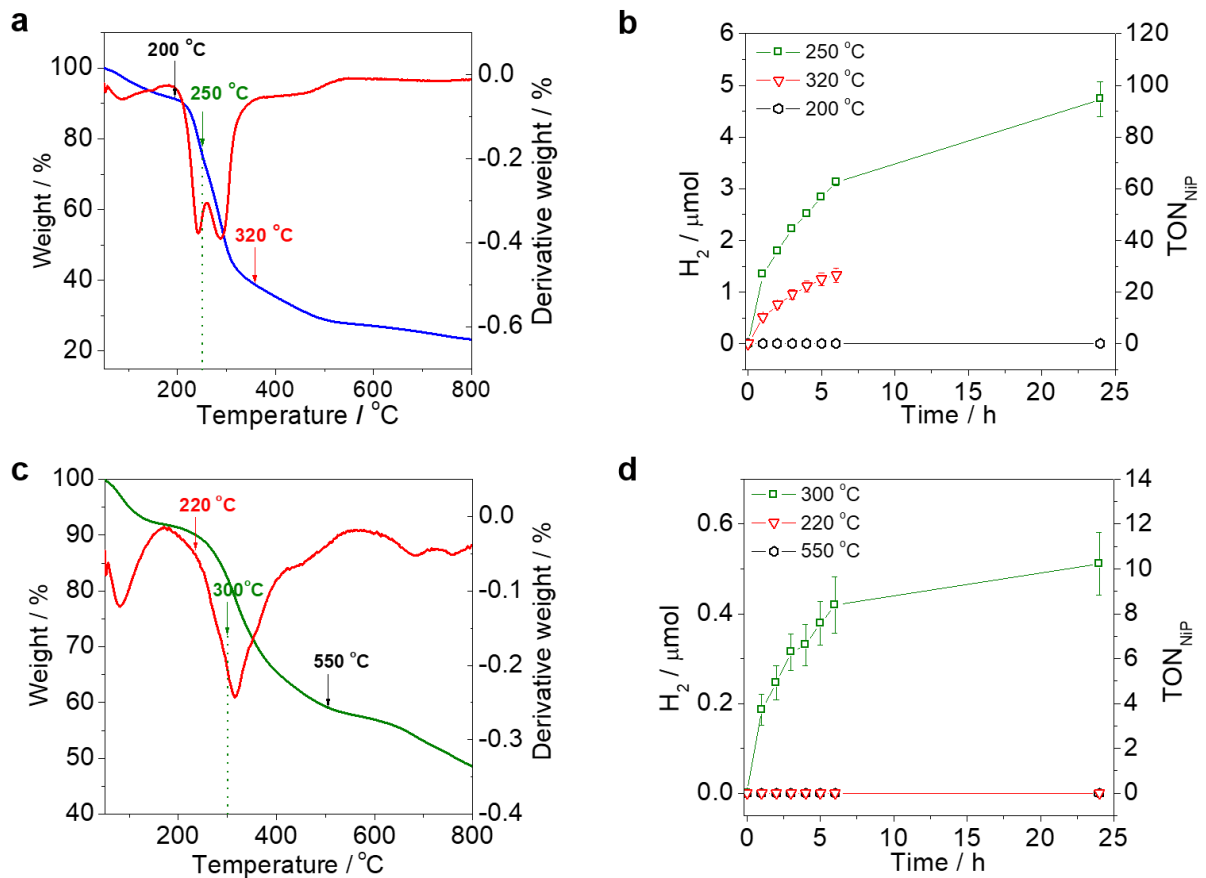


Figure S4. **a**, TGA thermogram (blue) and first TGA derivative (red) of xylan. The arrows show the temperatures at which the synthesis of the CDs was attempted. **b**, Photo-induced H_2 production from xylan-based photoabsorbers (2.2 mg) after calcination at 200, 250 and 320 °C for 4 days. **c**, TGA curve (green) and first TGA derivative (red) of lignin. The arrows indicate the temperatures that were tested for the synthesis of CDs. **d**, Light-induced H_2 production from lignin-derived light-harvesters (2.2 mg) upon calcination at 220, 300 and 550 °C for 4 days. Conditions for photocatalytic experiments; EDTA (0.1 M, pH 6, 3 mL) was used as sacrificial electron donor and **NiP** (50 nmol) as the H_2 evolution co-catalyst. The samples were tested under full solar light irradiation (AM 1.5 G, 100 mW cm⁻²), for 24 h, under N_2 atmosphere containing 2% CH_4 , at 25 °C.

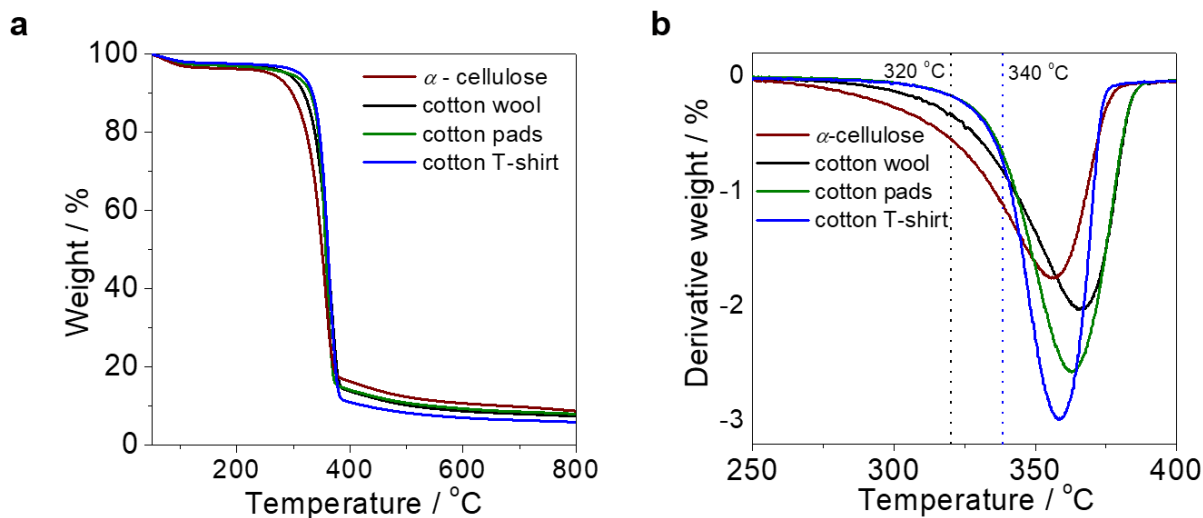


Figure S5. **a**, TGA thermograms and **b**, first TGA derivatives of cotton wool, pads and a T-shirt. Dotted lines show the temperatures at which the samples were decomposed for the synthesis of the carbonaceous materials. The TGA thermogram of α -cellulose is also overlaid with the cotton samples for comparison. Cotton wool was calcinated at 320 °C, similar to α -cellulose, whereas cotton pads and T-shirt at 340 °C, since their decomposition starts at higher temperatures. This is possibly due to the presence of some additives in the samples, used in textile industry (i.e. chemical defollients, metal salts and nanoparticulate metal oxides, such as ZnO, even pesticide traces).^{58, 59}

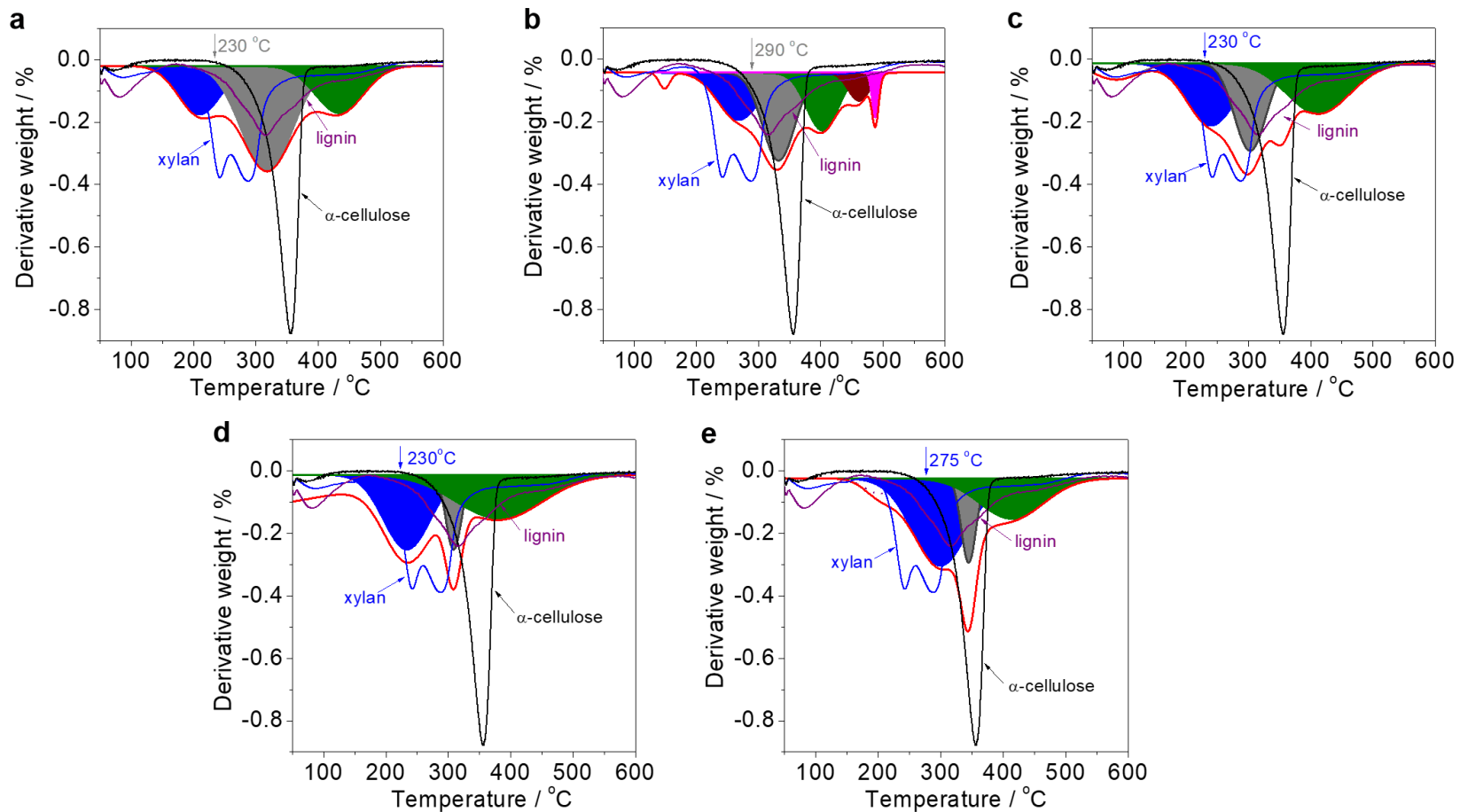


Figure S6. TGA first derivatives of **a**, *G. nivalis*, **b**, olive leaves, **c**, *G. elliptica*, **d**, *T. baccata* and **e**, *E. X. ebbingei*. Deconvoluted peaks attributed to xylan, α -cellulose and lignin, are shown in blue, grey and green, respectively. The additional wine and magenta bands in the TGA plot of olive leaves are attributed to polyphenols (antioxidants). TGA first derivatives of pure xylan, α -cellulose and lignin are shown with blue, black and purple solid lines, respectively, for reference. The arrows indicate the temperatures at which the samples were calcinated to synthesise the CDs from the leaves.

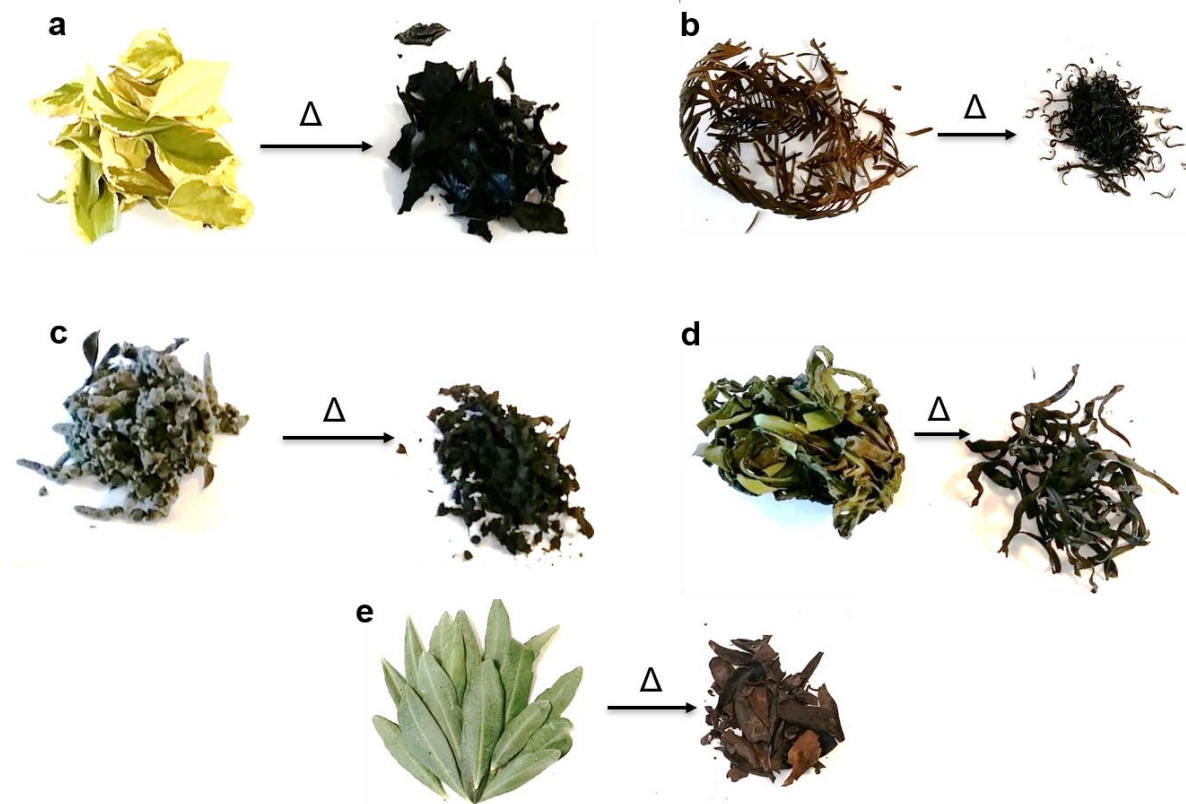


Figure S7. Photos of the crude biomass samples before (left) and after (right) calcination; **a**, *E. ebbingei*, **b**, *T. baccata*, **c**, *G. elliptica*, **d**, *G. nivalis* and **e**, olive leaves. Although the leaves changed colour and shrank after the controlled thermal treatment, they still maintained their shape and integrity.

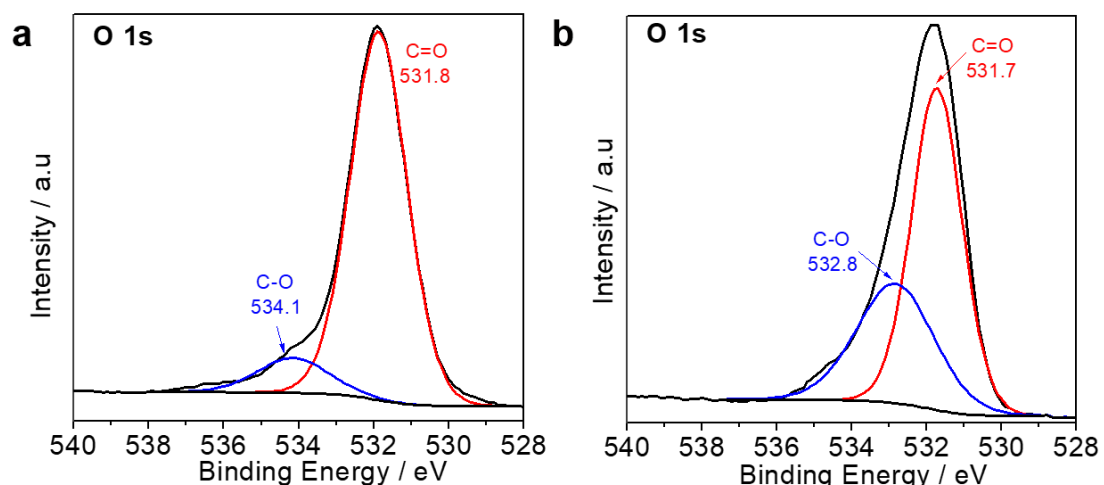


Figure S8. High resolution O 1s XPS spectra of **a**, α -cellulose and **b**, *G. nivalis* CDs deposited on fluorine-doped tin oxide (FTO) coated glass. The black lines represents the as recorded spectra, whereas the red and blue traces are the deconvoluted oxygen peaks.

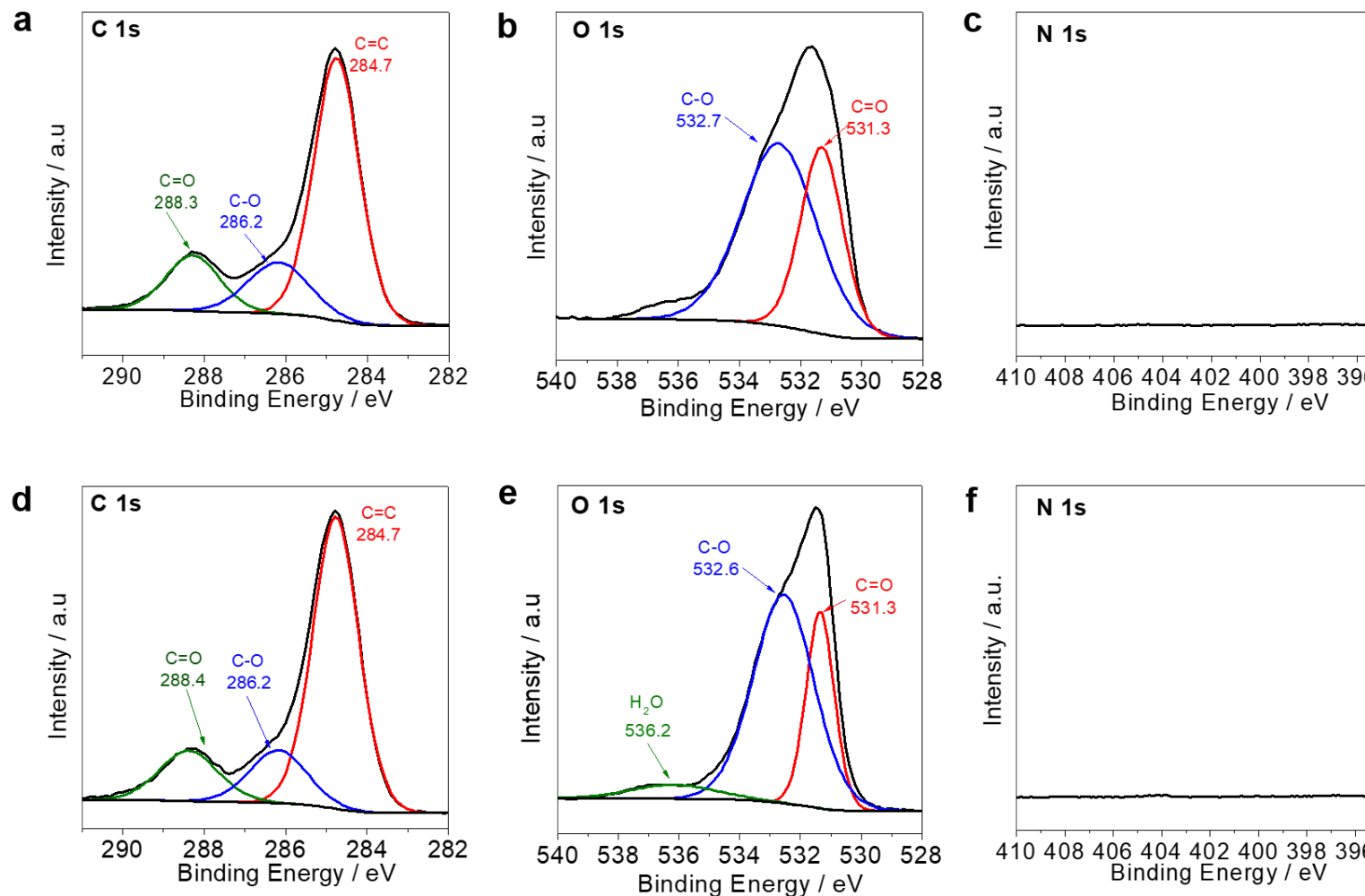


Figure S9. High resolution XPS spectra of xylan (**a**, C 1s, **b** O 1s and **c**, N 1s) and lignin-derived photoabsorbers (**d**, C 1s, **e**, O 1s and **f**, N 1s) measured on FTO coated glass. The black lines represent the as recorded spectra, whereas the red, blue and green traces are the deconvoluted bands for carbon and oxygen.

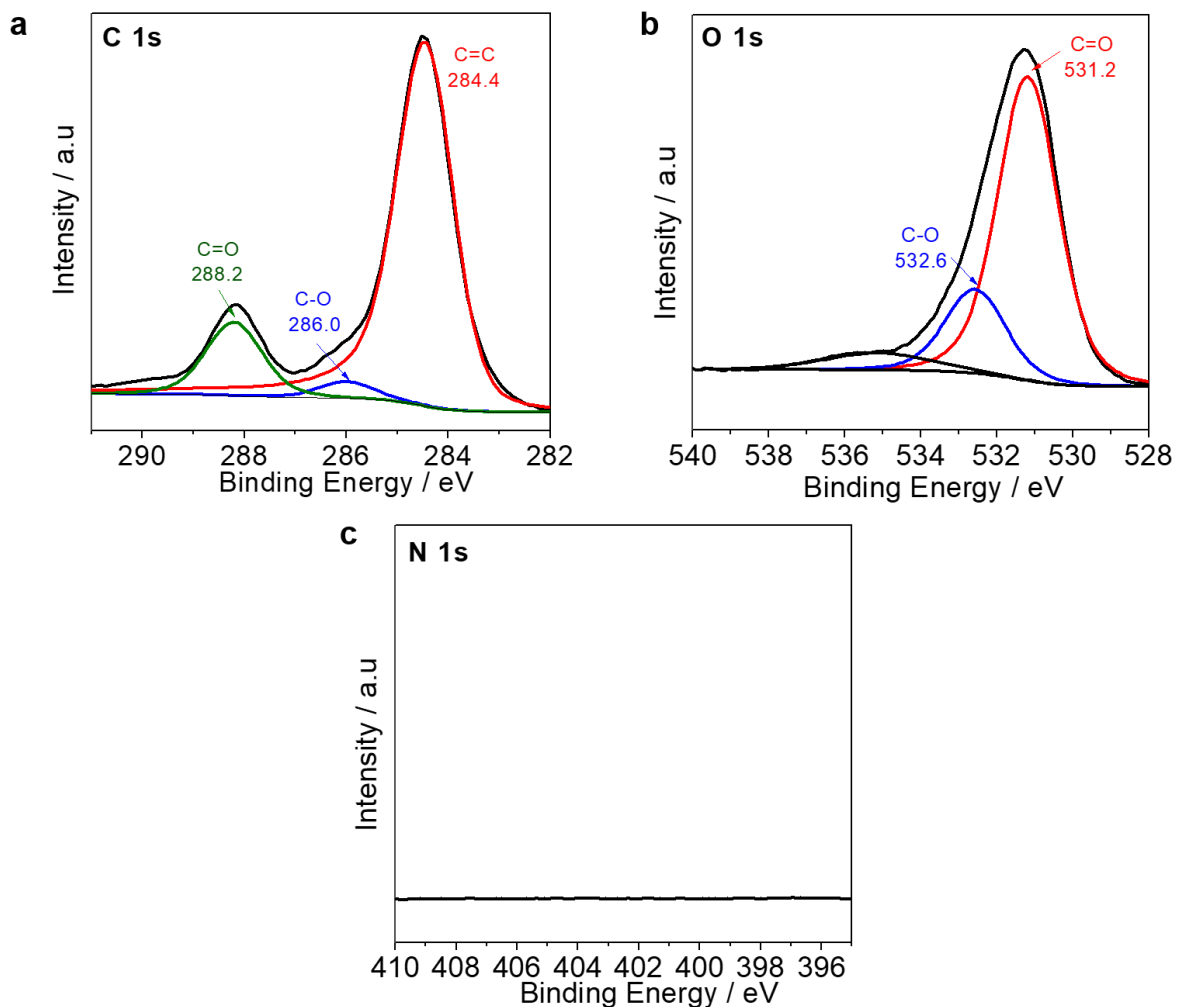


Figure S10. High resolution XPS data of CDs from cotton wool recorded on FTO coated glass; **a**, C 1s, **b**, O 1s and **c**, N 1s. The black lines show the spectra before deconvolution, whereas the red, green and blue lines are the deconvoluted bands for each element.

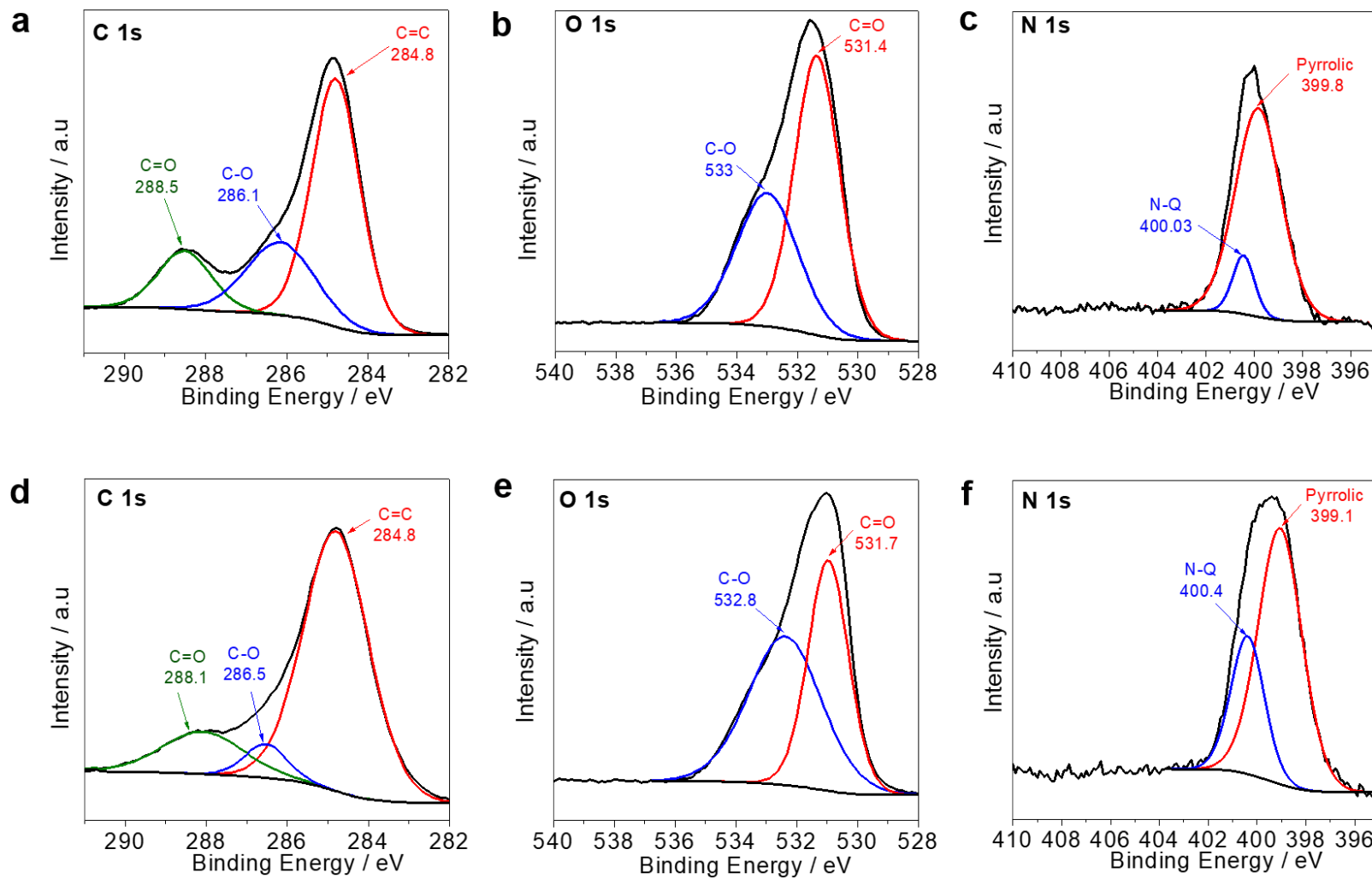


Figure S11. High resolution XPS spectra of *T. baccata* (**a**, C 1s, **b** O 1s and **c**, N 1s) and *E. X. ebbingei*-derived photoabsorbers (**d**, C 1s, **e**, O 1s and **f**, N 1s) recorded on FTO coated glass. The black lines correspond to the as recorded spectra, whereas the red, blue and green traces are the deconvoluted bands for all elements; carbon, oxygen and nitrogen.

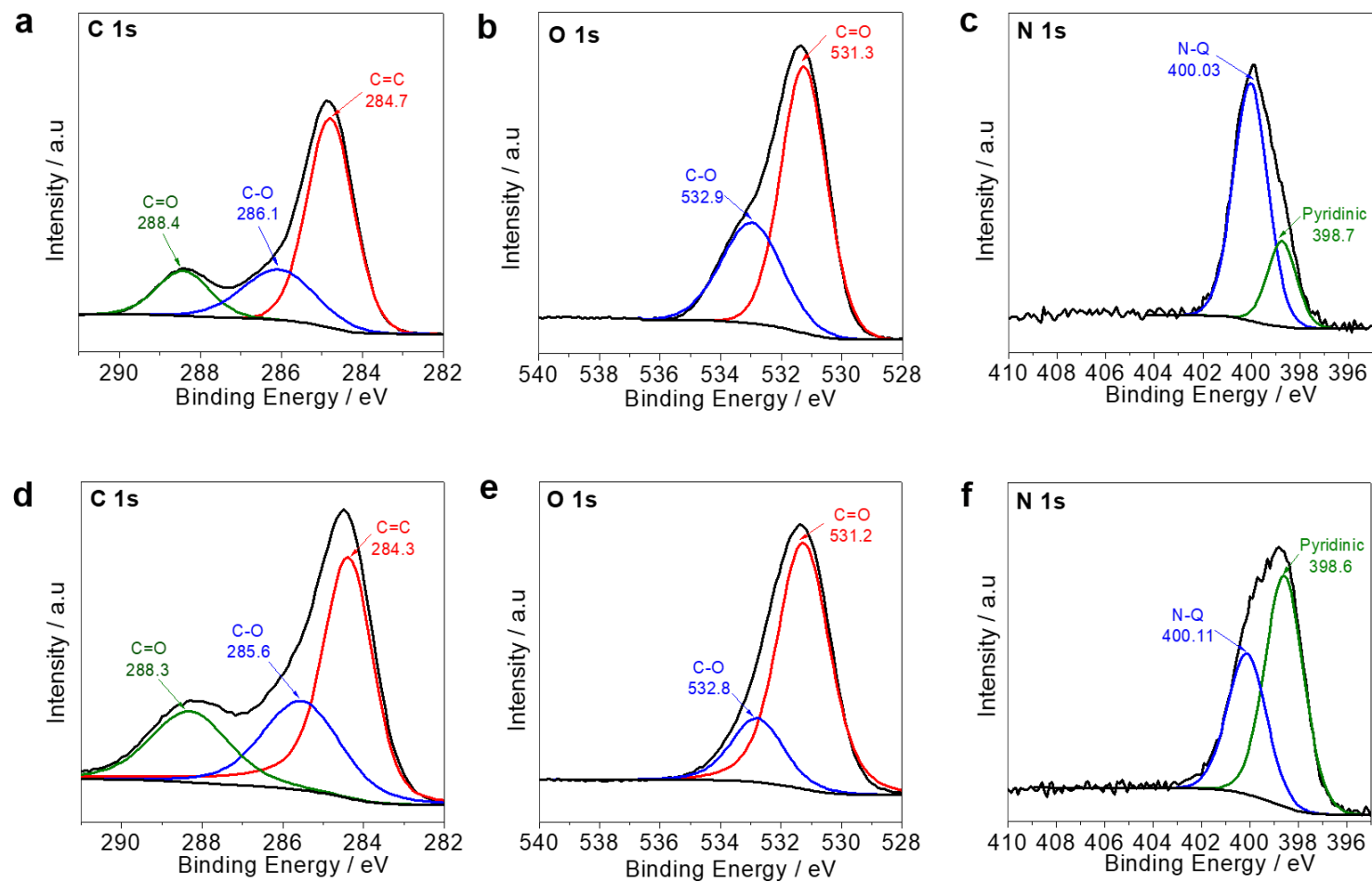


Figure S12. High resolution XPS spectra of *G. Elliptica* (**a**, C 1s, **b** O 1s and **c**, N 1s) and olive leaf-derived photoabsorbers (**d**, C 1s, **e**, O 1s and **f**, N 1s) obtained on FTO coated glass. The black lines show the as measured spectra, whereas the red, blue and green traces are the deconvoluted bands for carbon, oxygen and nitrogen.

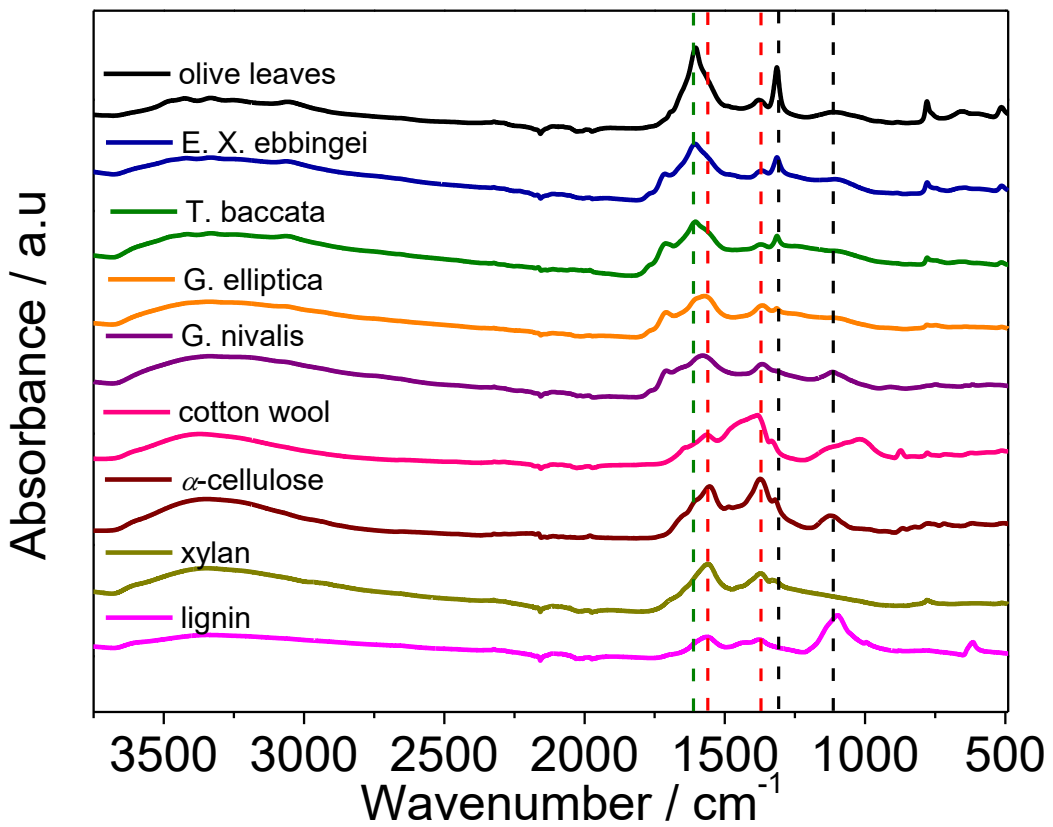


Figure S13. FTIR spectra of the carbonaceous photoabsorbers synthesised from lignin, xylan, α -cellulose, cotton wool, *G. nivalis*, *G. elliptica*, *T. baccata*, *E. X. ebbingei* and *olive leaves*. Dashed lines indicate the main vibrations observed; skeletal vibrations from graphitic core (1611 cm^{-1} , olive),⁶⁰ symmetric and anti-symmetric carboxylate stretches (1380 and 1560 cm^{-1} , respectively, red),^{51, 53} and $-\text{C-OH}$ stretching and $-\text{O-H}$ bending vibrations (1130 and 1319 cm^{-1} , respectively, black). $-\text{O-H}$ stretching vibrations are shown as a broad band between 3000 and 3500 cm^{-1} .⁶⁰

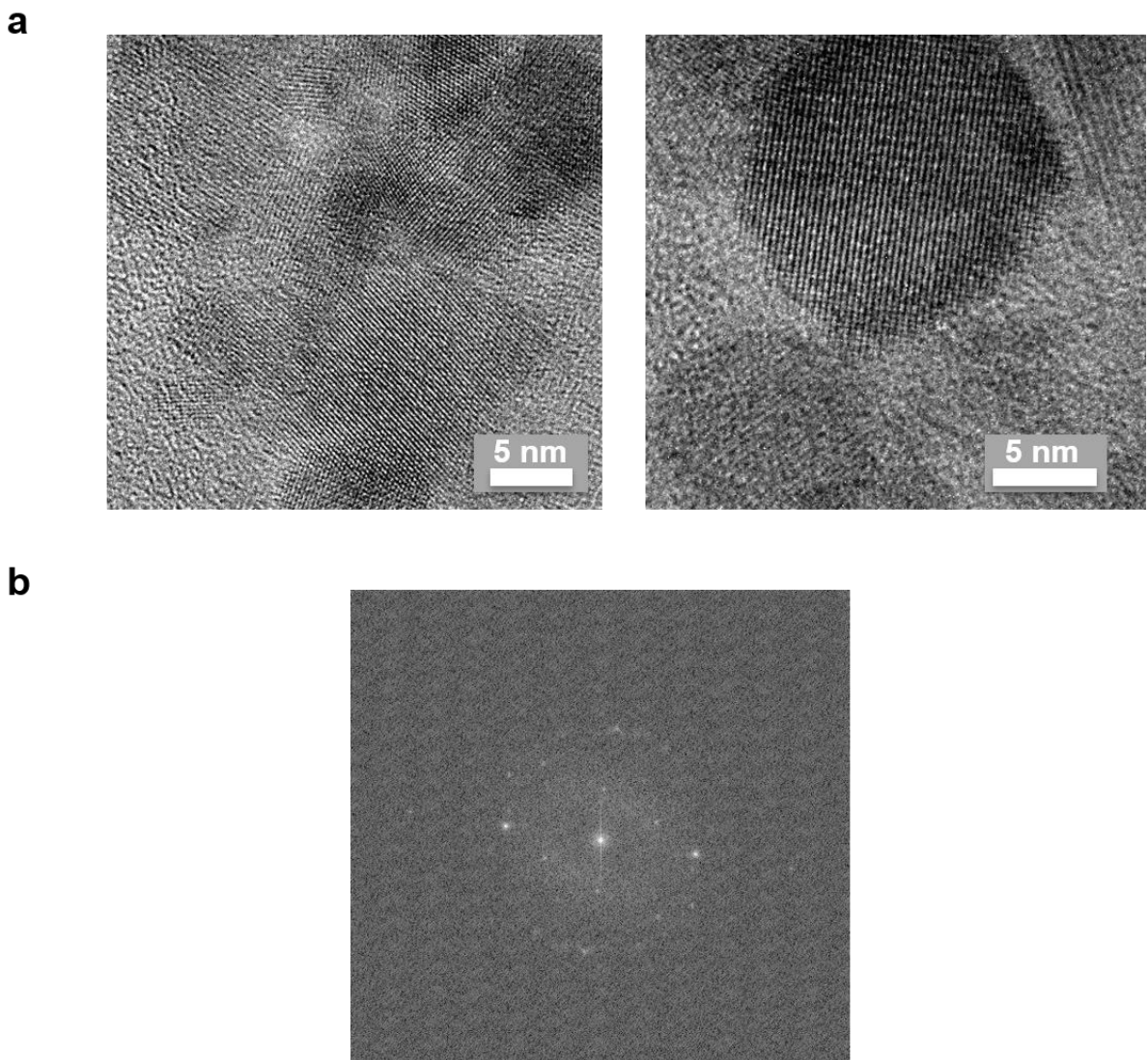


Figure S14. **a**, TEM images of a α -cellulose CDs at high magnifications, **b**, FFT image of α -cellulose CDs derived from **a**, used for the calculation of the (001) intralayer spacing (3.0 Å).

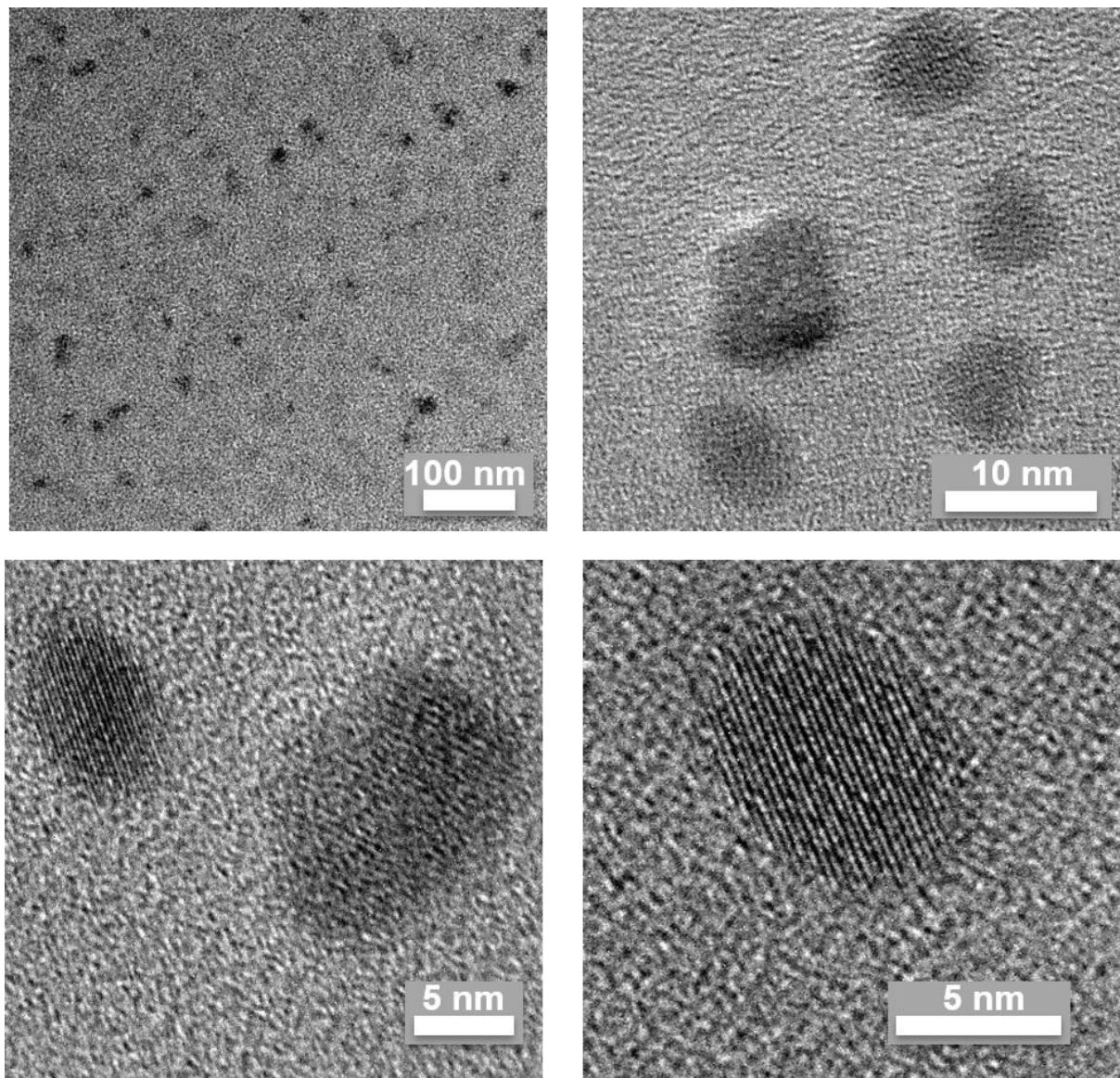
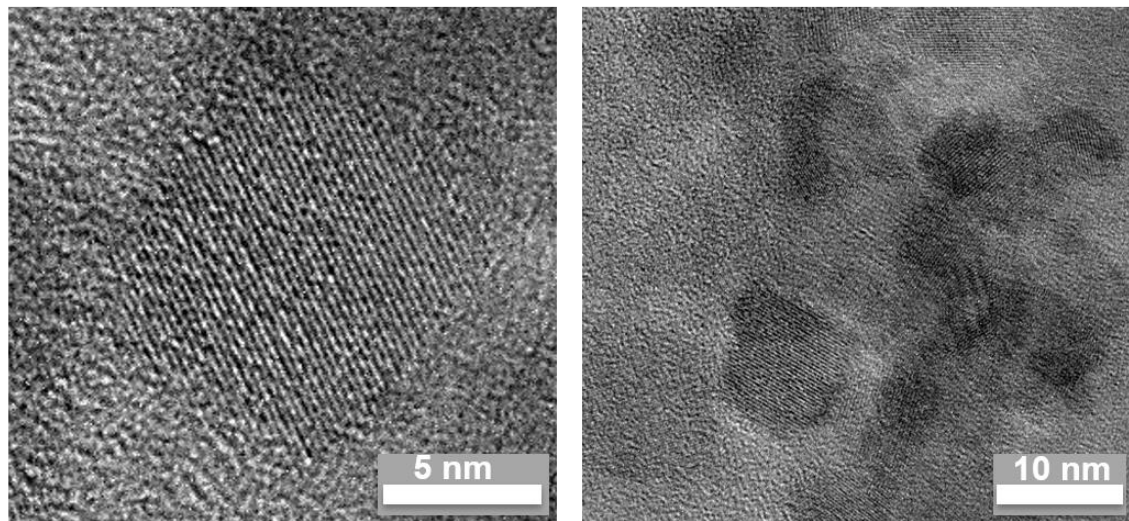


Figure S15. TEM images of CDs derived from *G. nivalis* at different magnifications. The bottom right image was used for the calculation of the (001) intralayer spacing (2.6 Å).

a



b

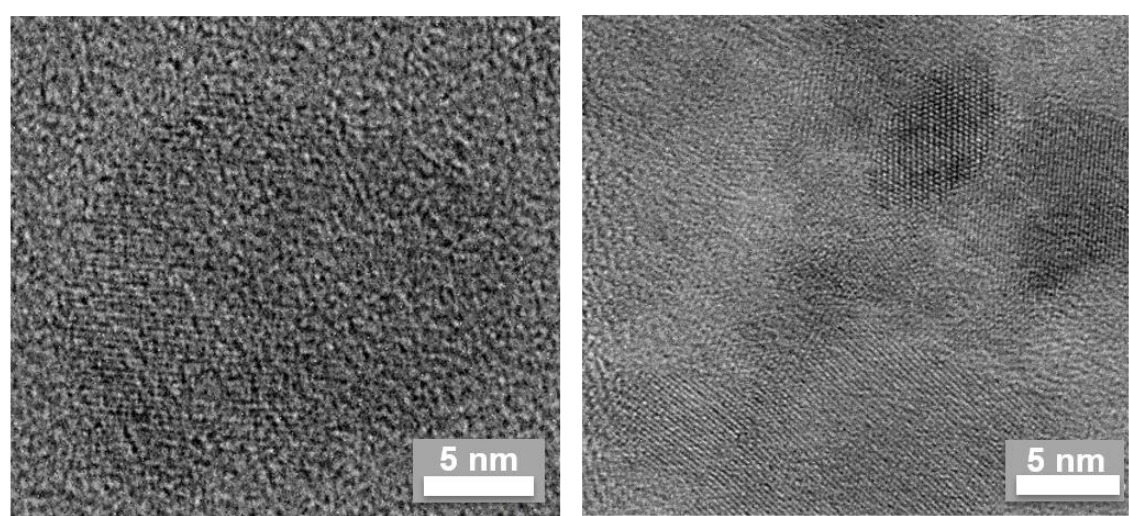


Figure S16. TEM images of photoabsorbers obtained from **a**, cotton wool and **b**, olive leaves.

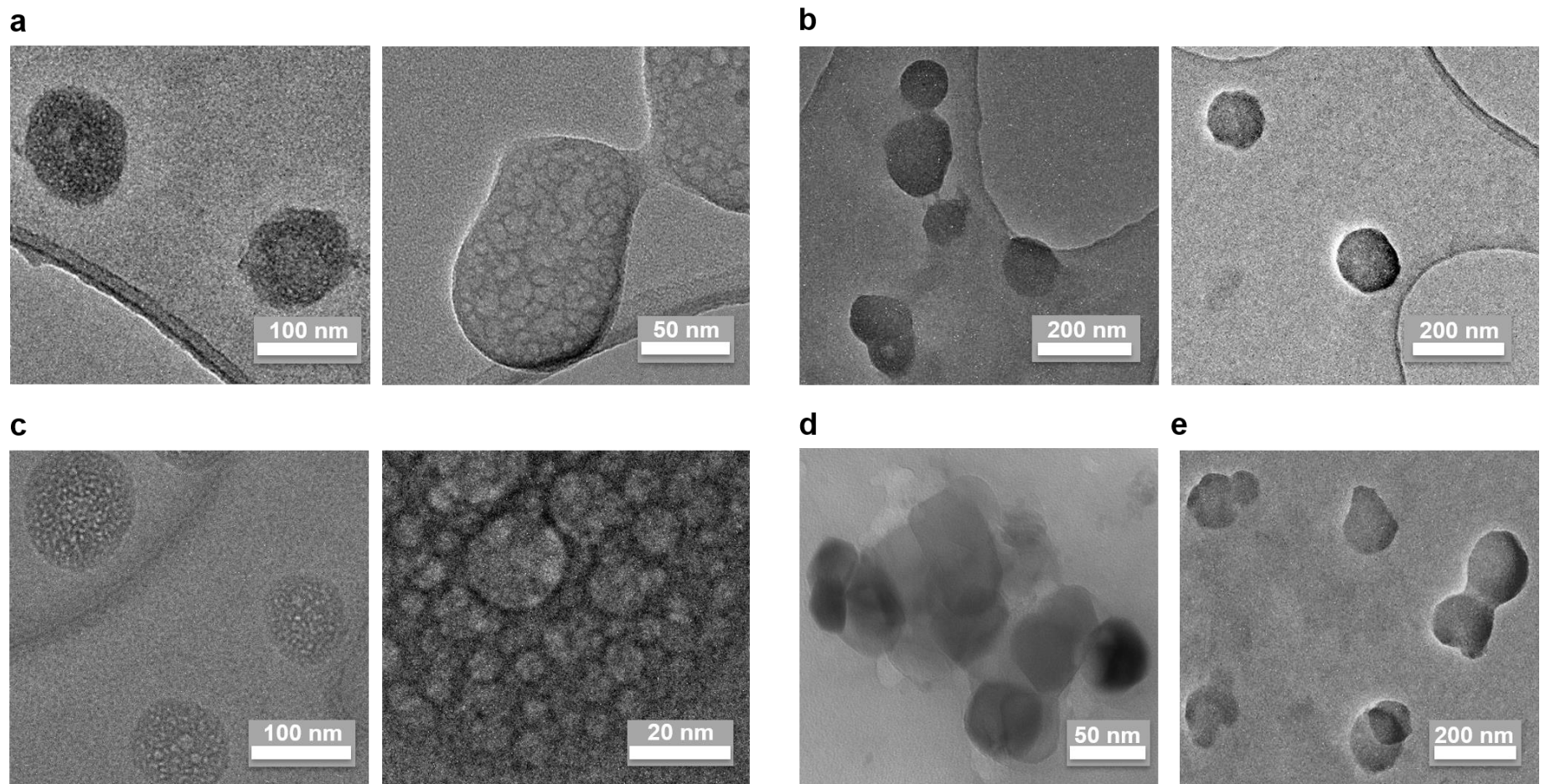


Figure S17. TEM images of carbonaceous light-harvesters synthesised from the biomass purified components, **a**, lignin and **b**, xylan, as well as waste biomass precursors, **c**, *G. elliptica*, **d**, *T. baccata*, and **e**, *E. X. ebbingei*.

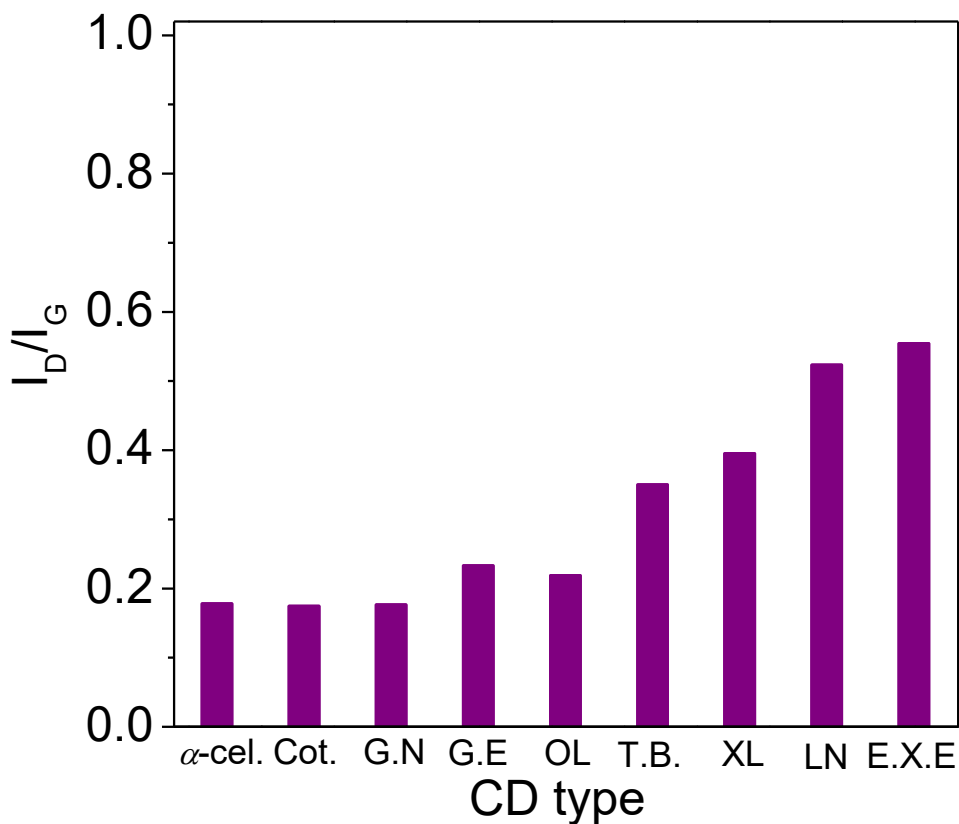


Figure S18. D to G band intensity ratios determined by Raman spectroscopy for the photoabsorbers derived from both purified and waste biomass precursors; α -cellulose (α -cel.), cotton wool (Cot.), *G. nivalis* (G. N), *G. elliptica* (G. E), olive leaves (OL), xylan (XL), lignin (LN) and *E. X. ebbingei* (E.X.E).

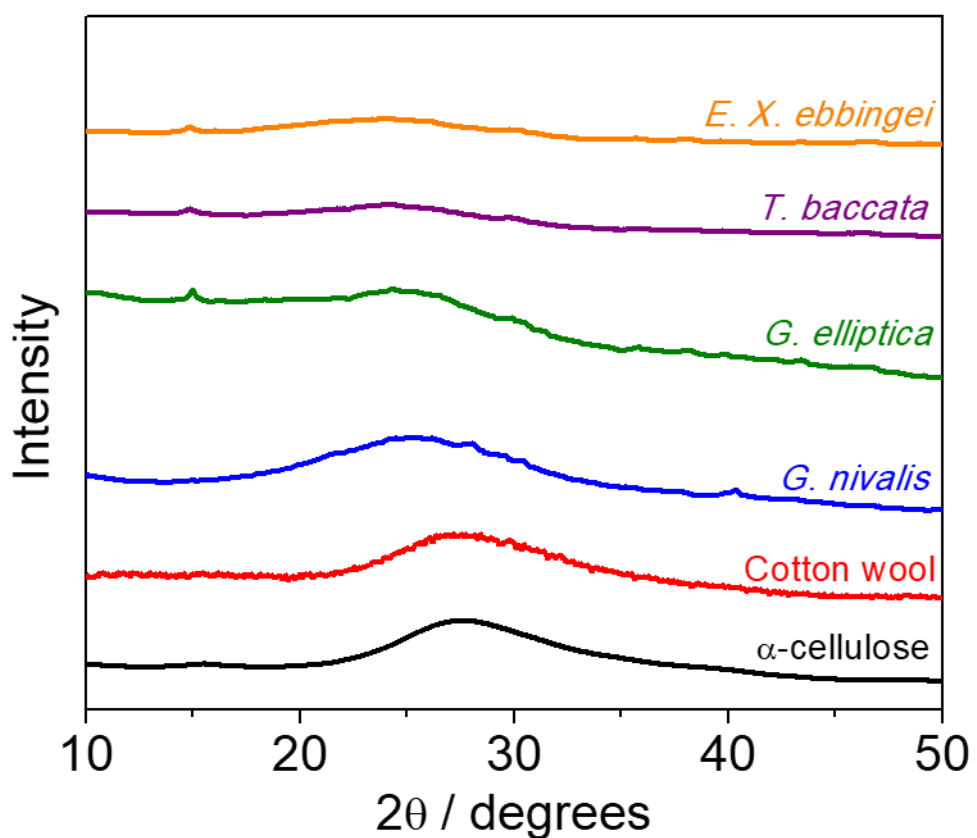


Figure S19. Powder XRD patterns of the photoabsorbers from α -cellulose, cotton wool, *G. nivalis*, *G. elliptica*, *T. baccata* and *E. X. ebbingei*.

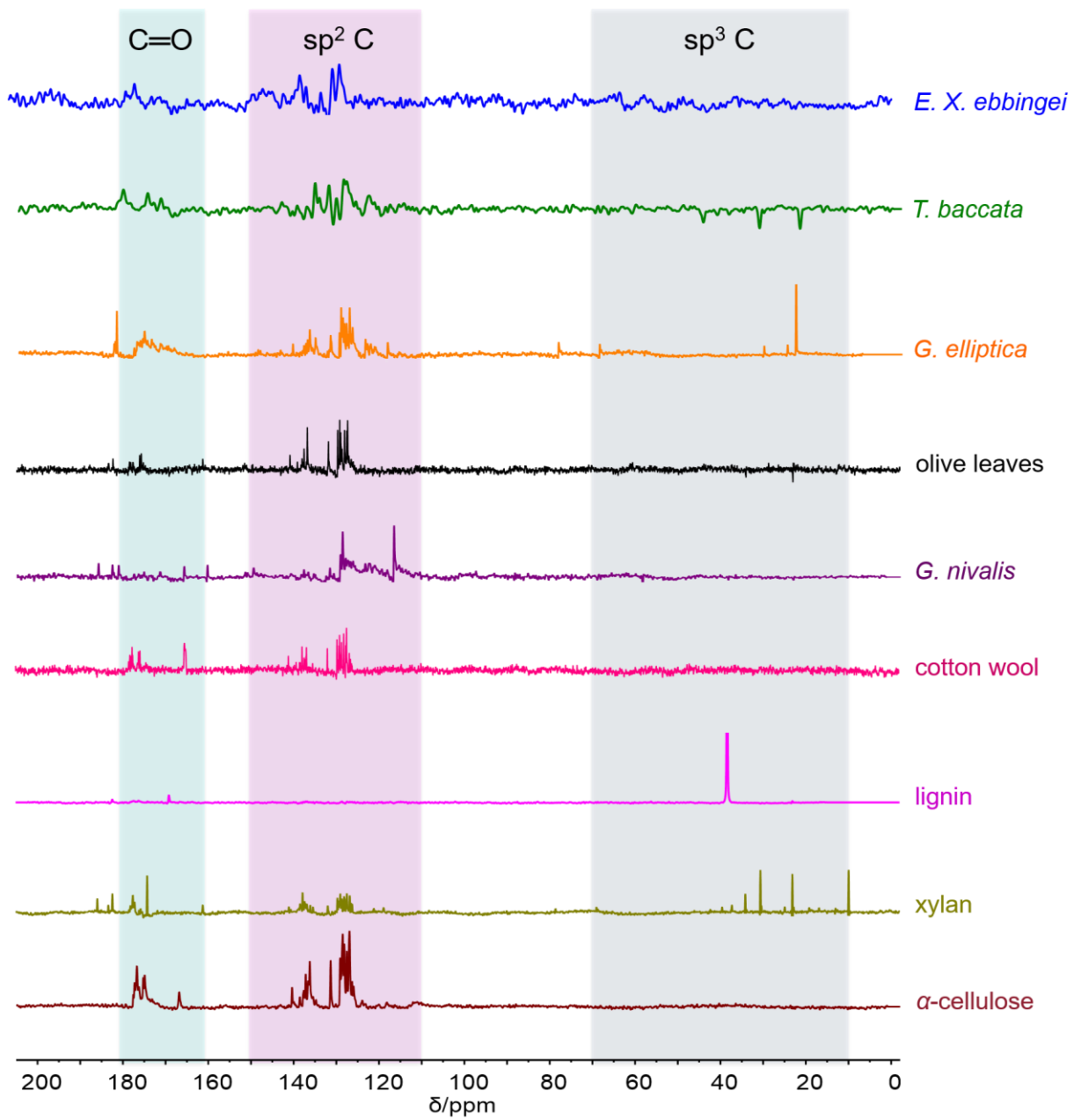


Figure S20. ^{13}C NMR spectra of the carbonaceous photoabsorbers synthesised from α -cellulose, xylan, lignin, cotton wool, *G. nivalis*, olive leaves, *G. elliptica*, *T. baccata* and *E. X. ebbingei* in D_2O .

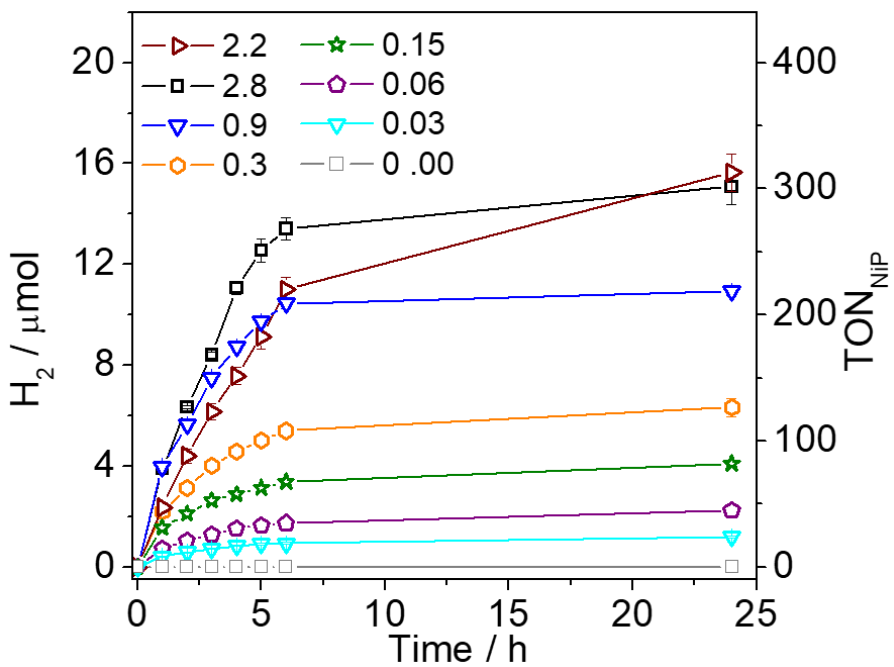


Figure S21. Solar-light driven H_2 evolution using α -cellulose CDs at various quantities (0.03–2.8 mg). All photocatalytic experiments were carried out at 50 nmol **NiP** and in aqueous EDTA solutions (0.1 M, pH 6, 3 mL), under full solar spectrum irradiation (AM 1.5 G, 100 mW cm⁻²) at 25 °C.

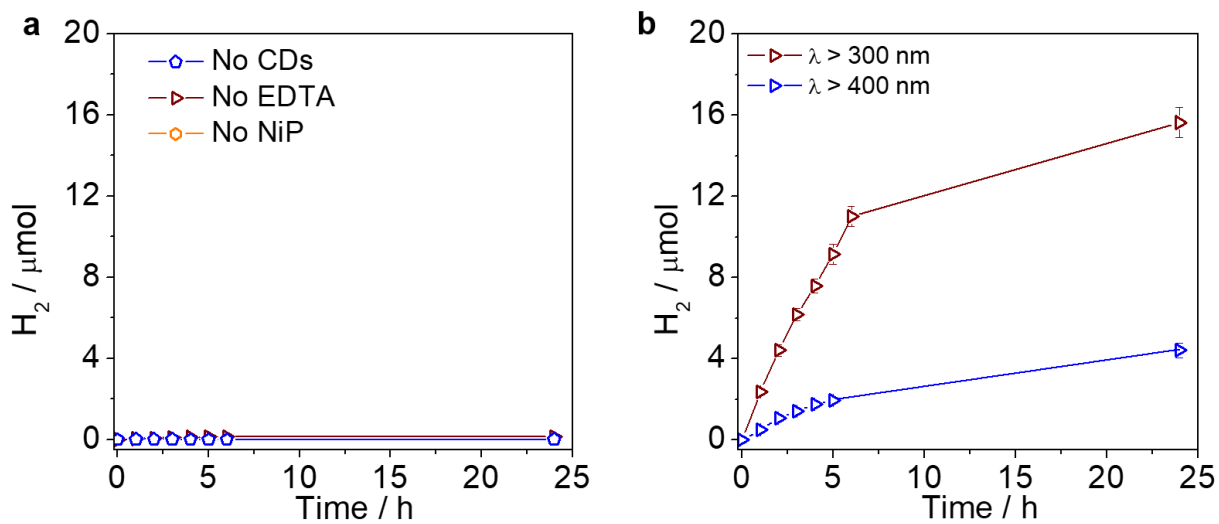


Figure S22. **a**, Control photocatalytic experiments in the absence of α -cellulose CDs, **NiP** and EDTA, carried out under full solar spectrum irradiation (AM 1.5 G, 100 mW cm⁻²), at 25 °C. **b**, Photocatalytic experiments using α -cellulose CDs (2.2 mg) in EDTA (0.1 M, pH 6, 3 mL), under full solar spectrum irradiation (AM 1.5 G, 100 mW cm⁻², $\lambda >$ 300 nm, wine), and in the presence of a longpass filter (blue) to restrict irradiation in the visible region of the solar spectrum ($\lambda >$ 400 nm). **NiP** (50 nmol) was used as the H_2 evolution catalyst in both cases.

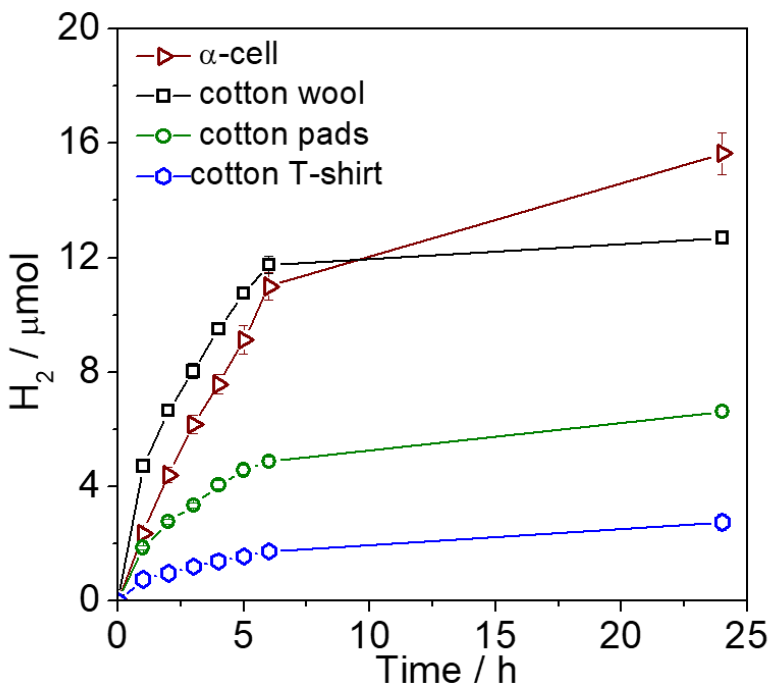


Figure S23. Solar-induced H_2 production using CDs (2.2. mg) from cotton as light-harvesters. Namely, cotton from different sources, such as cotton wool, pads and a T-shirt, were employed as precursors for this purpose. The photocatalytic experiments were carried out in aqueous EDTA solutions (0.1 M, pH 6, 3 mL), for 24 h, under full solar spectrum irradiation (AM 1.5 G, 100 mW cm^{-2}), in the presence of 50 nmol NiP, at 25 °C.

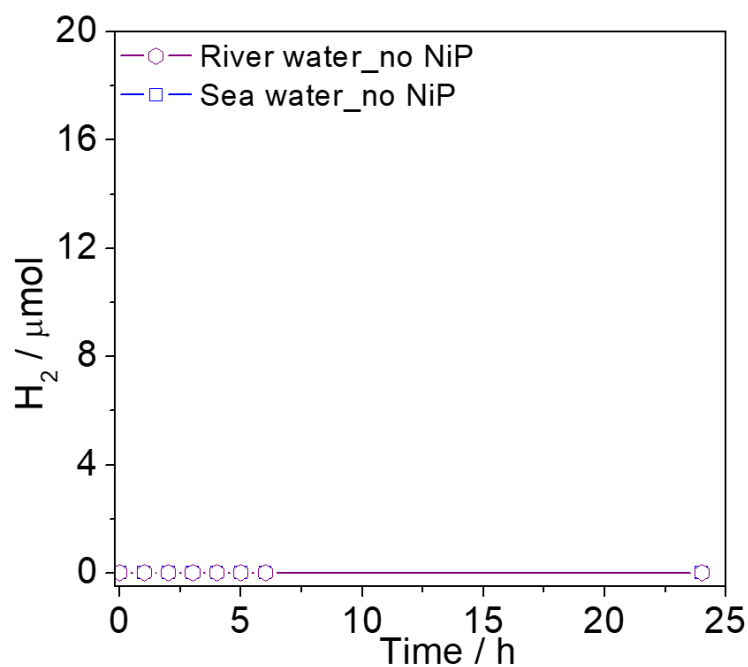


Figure S24. Control photocatalytic experiments in untreated river and sea water, without NiP, using α -cellulose CDs as photoabsorbers (2.2 mg) in the presence of EDTA (0.1 M, 3 mL, pH 6), after 24 h of irradiation (AM 1.5 G, 100 mW cm^{-2}), at 25 °C.

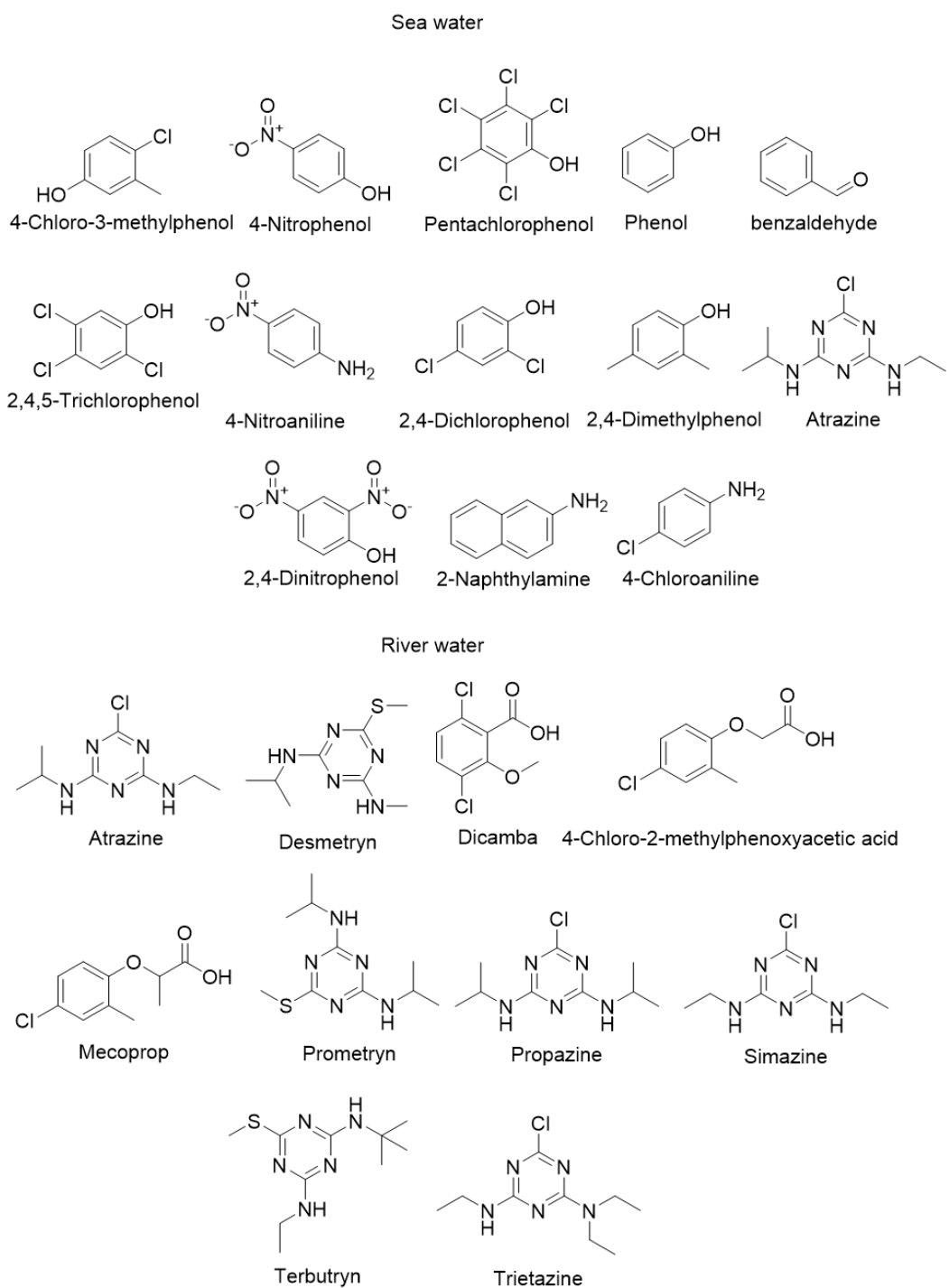


Figure S25. Chemical structures of organic water pollutants, which exist in sea (Gulf of Mexico) and river water (River Cam, UK), based on reports of the U. S. Department of Interior⁶¹ and the British environmental agency,⁶² respectively.

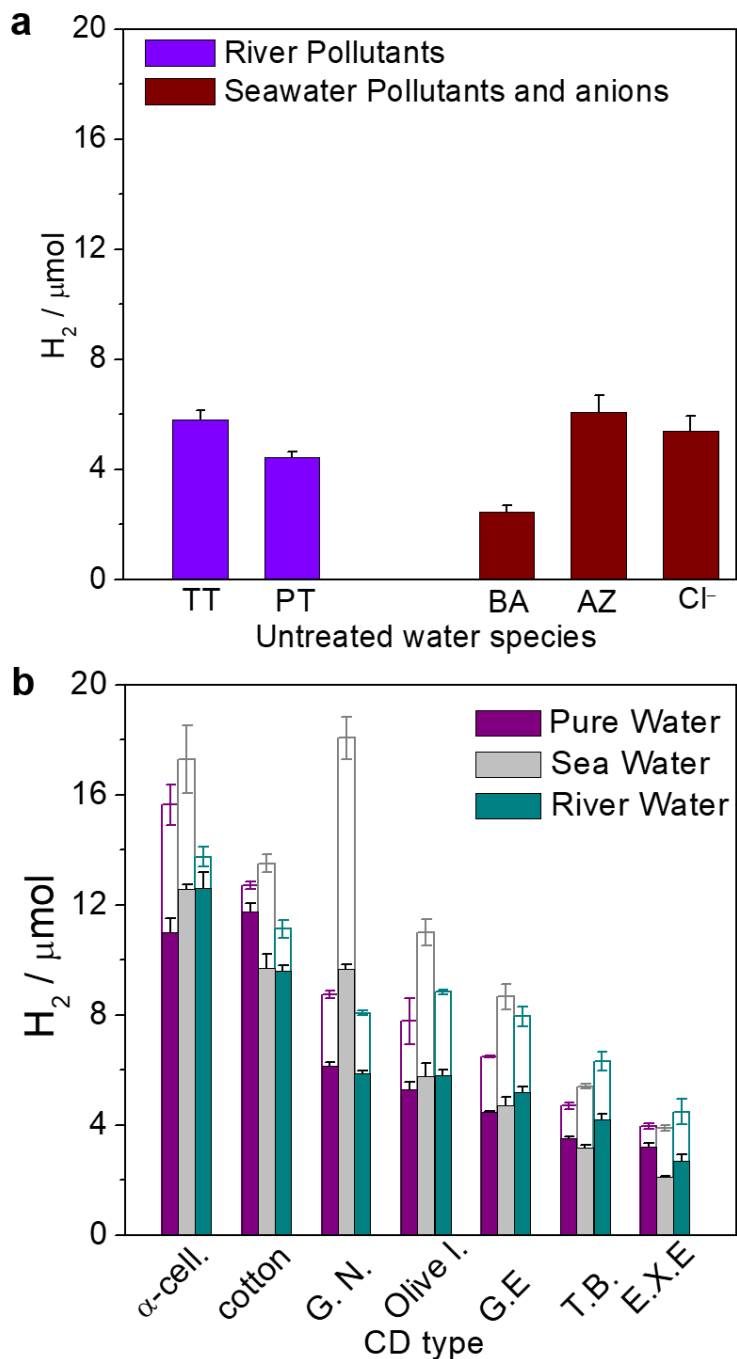


Figure S26. a, Photo-H₂ production (24 h) using α -cellulose CDs, in KPi (0.1 M, pH 6, 3 mL), without EDTA, but instead in the presence of the organic pollutants (200 μmol) terbutryl (TT), prometryn (PT), benzaldehyde (BA) and atrazine (AZ), as well as chloride anions (3.2 wt%), which all exist in sea and river water. **b**, Photo-H₂ production after 6 h (solid bars) and 24 h (empty bars) of irradiation using CDs from α -cellulose and crude biomass, in purified and untreated river and sea water, in the presence of EDTA (0.1 M, 3 mL, pH 6). Biomass waste samples; cotton wool (cotton), *G. Nivalis* (G. N.), olive leaves (Olive I.), *G. Elliptica* (G. E.), *T. Baccata* (T. B.) and *Elaeagnus X. Ebbingei* (E. X. E.). All experiments were carried out upon full solar light irradiation (AM 1.5 G, 100 mW cm⁻²) and under N₂ atmosphere (containing 2% CH₄), at 25 °C.

Supplementary References

- S1. J. Kim, J. Lee and W. Choi, *Chem. Commun.*, 2008, 756-758.
- S2. J. Kim, D. Monllor-Satoca and W. Choi, *Energy Environ. Sci.*, 2012, **5**, 7647-7656.
- S3. Y. Li, G. Lu and S. Li, *Appl. Catal. A*, 2001, **214**, 179-185.
- S4. X. J. Zheng, L. F. Wei, Z. H. Zhang, Q. J. Jiang, Y. J. Wei, B. Xie and M. B. Wei, *Int. J. Hydrogen Energy*, 2009, **34**, 9033-9041.
- S5. Z. Jiang, W. Wan, W. Wei, K. Chen, H. Li, P. K. Wong and J. Xie, *Appl. Catal. B*, 2017, **204**, 283-295.
- S6. V. M. Dascalaki, M. Antoniadou, G. Li Puma, D. I. Kondarides and P. Lianos, *Environ. Sci. Technol.*, 2010, **44**, 7200-7205.
- S7. Y. C. Nie, F. Yu, L. C. Wang, Q. J. Xing, X. Liu, Y. Pei, J. P. Zou, W. L. Dai, Y. Li and S. L. Suib, *Appl. Catal. B*, 2018, **227**, 312-321.
- S8. A.-J. Simamora, F.-C. Chang, H. P. Wang, T.-C. Yang, Y.-L. Wei and W.-K. Lin, *Int. J. Photoenergy*, 2013, **2013**, 419182.
- S9. A. E. Lanterna and J. C. Scaiano, *ACS Energy Lett.*, 2017, **2**, 1909-1910.
- S10. K. Li, Z. Zeng, L. Yan, M. Huo, Y. Guo, S. Luo and X. Luo, *Appl. Catal., B*, 2016, **187**, 269-280.
- S11. L. Guo, Z. Yang, K. Marcus, Z. Li, B. Luo, L. Zhou, X. Wang, Y. Du and Y. Yang, *Energy Environ. Sci.*, 2018, **11**, 106-114
- S12. B. C. Hodges, E. L. Cates and J.-H. Kim, *Nat. Nanotechnol.*, 2018, **13**, 642-650.
- S13. D. Lu, H. Wang, X. Zhao, K. K. Kondamareddy, J. Ding, C. Li and P. Fang, *ACS Sustainable Chem. Eng.*, 2017, **5**, 1436-1445.
- S14. H. Liu, Z. Jin, Z. Xu, Z. Zhang and D. Ao, *RSC Adv.*, 2015, **5**, 97951-97961.
- S15. Y. Wu, H. Wang, W. Tu, S. Wu, Y. Liu, Y. Z. Tan, H. Luo, X. Yuan and J. W. Chew, *Appl. Catal. B*, 2018, **229**, 181-191.
- S16. C. H. Choi, L. Lin, S. Gim, S. Lee, H. Kim, X. Wang and W. Choi, *ACS Catal.*, 2018, **8**, 4241-4256.
- S17. Y. Wu, H. Wang, W. Tu, Y. Liu, S. Wu, Y. Z. Tan and J. W. Chew, *Appl. Catal. B*, 2018, **233**, 58-69.
- S18. L. N. Qiao, H. C. Wang, Y. D. Luo, H. M. Xu, J. P. Ding, S. Lan, Y. Shen, Y. H. Lin and C. W. Nan, *J. Am. Ceram. Soc.*, 2018, **101**, 3015-3025.
- S19. H. Fu, L. Yang, D. Hu, C. Yu, Y. Ling, Y. Xie, S. Li and J. Zhao, *Int. J. Hydrg. Energy*, 2018, **43**, 10359-10367.
- S20. P. Tian, X. He, W. Li, L. Zhao, W. Fang, H. Chen, F. Zhang, W. Zhang and W. Wang, *J. Mater. Sci.*, 2018, **53**, 12016-12029.
- S21. Q. Wang, B. Geng and S. Wang, *Environ. Sci. Technol.*, 2009, **43**, 8968-8973.
- S22. J. Senthilnathan and L. Philip, *Water Air Soil Pollut.*, 2010, **210**, 143-154.
- S23. N. M. Mahmoodi and M. Arami, *J. Alloy. Comp.*, 2010, **506**, 155-159.
- S24. X. Zhou, C. Hu, X. Hu, T. Peng and J. Qu, *J. Phys. Chem. C*, 2010, **114**, 2746-2750.

- S25. V. Belessi, D. Lambropoulou, I. Konstantinou, R. Zboril, J. Tucek, D. Jancik, T. Albanis and D. Petridis, *Appl. Catal. B*, 2009, **87**, 181-189.
- S26. L. Yin, J. Niu, Z. Shen and J. Chen, *Environ. Sci. Technol.*, 2010, **44**, 5581-5586.
- S27. H. Yu, X. Wang, H. Sun and M. Huo, *J. Hazard. Mater.*, 2010, **184**, 753-758.
- S28. A. Hu, X. Zhang, K. D. Oakes, P. Peng, Y. N. Zhou and M. R. Servos, *J. Hazard. Mater.*, 2011, **189**, 278-285.
- S29. H. Chen, S. Yang, K. Yu, Y. Ju and C. Sun, *J. Phys. Chem. A*, 2011, **115**, 3034-3041.
- S30. L. Xuanhua, C. Guangyu, Y. Liangbao, J. Zhen and L. Jinhuai, *Adv. Funct. Mater.*, 2010, **20**, 2815-2824.
- S31. A. Gajović, A. M. T. Silva, R. A. Segundo, S. Šturm, B. Jančar and M. Čeh, *Appl. Catal. B*, 2011, **103**, 351-361.
- S32. R. K. Das, J. P. Kar and S. Mohapatra, *Ind. Eng. Chem. Res.*, 2016, **55**, 5902-5910.
- S33. B. Y. Yu and S.-Y. Kwak, *J. Mater. Chem.*, 2012, **22**, 8345-8353.
- S34. J. Di, J. Xia, Y. Ge, H. Li, H. Ji, H. Xu, Q. Zhang, H. Li and M. Li, *Appl. Catal. B*, 2015, **168-169**, 51-61.
- S35. G.-W. Cui, W.-I. Wang, M.-y. Ma, M. Zhang, X.-y. Xia, F.-y. Han, X.-f. Shi, Y.-q. Zhao, Y.-B. Dong and B. Tang, *Chem. Commun.*, 2013, **49**, 6415-6417.
- S36. H. Zhang, L. Zhao, F. Geng, L.-H. Guo, B. Wan and Y. Yang, *Appl. Catal. B*, 2016, **180**, 656-662.
- S37. S. Hu, Y. Ding, Q. Chang, J. Yang and K. Lin, *Appl. Surf. Sci.*, 2015, **355**, 774-777.
- S38. B. Lin, G. Yang, B. Yang and Y. Zhao, *Appl. Catal. B*, 2016, **198**, 276-285.
- S39. M. Tahir, C. Cao, N. Mahmood, F. K. Butt, A. Mahmood, F. Idrees, S. Hussain, M. Tanveer, Z. Ali and I. Aslam, *ACS Appl. Mater. Interfaces*, 2014, **6**, 1258-1265.
- S40. Y. Cui, J. Huang, X. Fu and X. Wang, *Catal. Sci. Technol.*, 2012, **2**, 1396-1402.
- S41. L. Ge, C. Han and J. Liu, *J. Mater. Chem.*, 2012, **22**, 11843-11850.
- S42. S. C. Yan, Z. S. Li and Z. G. Zou, *Langmuir*, 2010, **26**, 3894-3901.
- S43. C. Liu, L. Jing, L. He, Y. Luan and C. Li, *Chem. Commun.*, 2014, **50**, 1999-2001.
- S44. K. S. Yeon, O. Junghoon, P. Sunghee, S. Yeonjun and P. Sungjin, *Chem. Eur. J.*, 2016, **22**, 5142-5145.
- S45. H. Yang, W. Zhenhai, C. Shumao, G. Xiaoru and C. Junhong, *Adv. Mater.*, 2013, **25**, 6291-6297.
- S46. Z.-R. Tang, Y. Zhang, N. Zhang and Y.-J. Xu, *Nanoscale*, 2015, **7**, 7030-7034.
- S47. G. M. Neelgund, V. N. Bliznyuk and A. Oki, *Appl. Catal. B*, 2016, **187**, 357-366.
- S48. Z. Shen, Z. Hu, W. Wang, S.-F. Lee, D. K. L. Chan, Y. Li, T. Gu and J. C. Yu, *Nanoscale*, 2014, **6**, 14163-14167.
- S49. S. A. Ansari and M. H. Cho, *Sci. Rep.*, 2016, **6**, 25405.
- S50. S. Ahmed, M. G. Rasul, R. Brown and M. A. Hashib, *J. Environ. Manag.*, 2011, **92**, 311-330.

- S51. B. C. M. Martindale, G. A. M. Hutton, C. A. Caputo and E. Reisner, *J. Am. Chem. Soc.*, 2015, **137**, 6018-6025.
- S52. B. C. M. Martindale, E. Joliat, C. Bachmann, R. Alberto and E. Reisner, *Angew. Chem. Int. Ed.*, 2016, **55**, 9402-9406.
- S53. B. C. M. Martindale, G. A. M. Hutton, C. A. Caputo, S. Prantl, R. Godin, J. R. Durrant and E. Reisner, *Angew. Chem. Int. Ed.*, 2017, **56**, 6459-6463.
- S54. P. Yang, J. Zhao, J. Wang, H. Cui, L. Li and Z. Zhu, *ChemPhysChem*, 2015, **16**, 3058-3063.
- S55. C. A. Caputo, M. A. Gross, V. W. Lau, C. Cavazza, B. V. Lotsch and E. Reisner, *Angew. Chem. Int. Ed.*, 2014, **53**, 11538-11542.
- S56. H. Kasap, C. A. Caputo, B. C. M. Martindale, R. Godin, V. W.-h. Lau, B. V. Lotsch, J. R. Durrant and E. Reisner, *J. Am. Chem. Soc.*, 2016, **138**, 9183-9192.
- S57. D. J. Martin, K. Qiu, S. A. Shevlin, A. D. Handoko, X. Chen, Z. Guo and J. Tang, *Angew. Chem. Int. Ed.*, 2014, **53**, 9240-9245.
- S58. R. H. Barker, *Environ. Health. Perspect.*, 1975, **11**, 41-45.
- S59. P. J. Rivero, A. Urrutia, J. Goicoechea and F. J. Arregui, *Nanoscale Res. Lett.*, 2015, **10**, 501.
- S60. G. Yang, G. Zhang, P. Sheng, F. Sun, W. Xu and D. Zhang, *J. Mater. Chem.*, 2012, **22**, 4391-4395.
- S61. L. H. Nowell, A. S. Ludtke, D. K. Mueller and J. C. Scott, *USGS open-file report* 2011-1271.
- S62. K. Brown, *River Cam water quality data, British environmental agency*, 2017.

End of Electronic Supporting Information